Comparative study between S-N and fracture mechanics approach on reliability assessment of offshore wind turbine jacket foundations

Abdulhakim Adeoye Shittu[1,2], Ali Mehmanparast[1], Phil Hart[1], Athanasios Kolios[3]

[1]Energy and Power Theme, Cranfield University, Cranfield, Bedfordshire MK43 0AL, United Kingdom

[2]Department of Mathematics and Statistics, Federal University Wukari, Taraba P.M.B. 1020, Nigeria

[3]Department of Naval Architecture, Ocean and Marine Engineering, University of Strathclyde, Glasgow G1 1XQ, United Kingdom

Abstract

This paper investigates from a structural reliability assessment (SRA) perspective the fatigue reliability using the S-N curve approach compared with the fracture mechanics (FM) approach for a typical welded offshore wind turbine (OWT) jacket support structures. A non-intrusive formulation was developed for an OWT jacket support structure in 50 m deep water, consisting of a sequence of steps. First, stochastic parametric 3D (three-dimensional) Finite Element Analysis (FEA) simulations are performed, taking into account stochastic variables such as wind loads, wave loads and soil properties using facilities within the software package ANSYS. Secondly, the FEA results are post-processed using an Artificial Neural Network (ANN) response surface modelling technique deriving the performance functions expressed in terms of stochastic variables. Finally, the First Order Reliability Method (FORM) is applied in calculating the reliability index values of components. The developed framework was applied to elucidate the fatigue damage process, including the small to long crack transition among other stages, for structural steels used for OWT jacket applications. The FM formulation investigated includes a crack growth formulation based on the bilinear crack growth law, considering both segments of the crack growth law as non-correlated and correlated in calculating the reliability index (RI). Sensitivity analysis results showed a strong dependence of the structure's reliability levels on the uncertainties of the crack growth law constants measured in terms of coefficient of variation (COV). Also investigated, was the reliability of the structure reassessed and updated in the presence of assumed structural health monitoring/ condition monitoring (SHM/CM) data. The results from the case study revealed that fracture reliability is highly sensitive to the initial crack size. It is recommended to apply the S-N curve method at the design stage while the FM approach applied towards the end of the design life as the structure approaches failure.

Keywords: Fatigue, reliability index, non-intrusive formulations, crack growth, offshore wind structures, artificial neural network

1 Introduction

By 2030, it was projected that a large contribution of wind energy capacity could come from offshore wind farms in the EU [1]. Offshore wind farms are favoured due to higher wind speeds, unrestricted space, and lower marine environmental impact [2]. These conditions have led to an increase in wind farm installations in Europe, particularly in the North Sea, Irish Sea and Baltic Sea. A complete offshore wind turbine (OWT) consists of the wind turbine itself, installed on top of a support structure, which is resting on a foundation that is fixed in the soil. There are a number of different types of

support structures; these are selected depending on the water depth, the environmental loads, the cost of production and installation, complexity of the design, etc. [2–4].

A majority of OWTs use monopile foundations, especially when installed in water depths of less than 50 m. But for larger wind turbines, monopiles become very large and impractical. Hence, space frame structures such as jackets are used instead, since they are more light-weight and stiffer than monopiles. Space frames can also be cheaper in deepwater circumstances. However, the design of space frames is time-consuming, especially if it is desired to withstand a wide set of dynamic loads. Thus, more efforts are needed to improve the design and analysis of jacket-type support structures [5,6], considering as well the optimisation needed to manufacture them in large volumes [7,8].

To design offshore structures effectively, fatigue damage is an important limit state criterion to consider because materials with higher static strength must now be introduced. Historically, the aircraft industry was the first to introduce fatigue as a criterion for design, followed by other industries such as nuclear, steel, offshore, and shipping. In the latter, the fatigue limit state (FLS) had to be explicitly defined, precisely because higher strength steels were used in the design. Usually, the S-N data are first obtained from laboratory experiments, which serve as basis for the design criteria against fatigue failure. Besides good design, in-service inspection, maintenance and repair (IMR), is needed to keep adequate structural safety and system integrity during the service life. This has led to the development of fracture mechanics (FM) and reliability-based methods to assess crack growth in any structure. The FM approach is essential for understanding the relationship between different parameters and uncertainties involved in the fatigue damage process [9].

S-N curves have been applied extensively to do fatigue design checks under complex loading conditions. Inspection and repair can, in addition to safeguarding against fatigue failure, be used to increase the reliability in view of crack growth. More information about crack growth than obtained from S-N data are required in order to support inspection planning. Besides describing the gradual development of crack, the FM is also a potential tool which could account for the effect of structural health monitoring/condition monitoring (SHM/CM) data. As a result of the inherent uncertainties of the crack growth method and data, reliability methods can be used to support subsequent decisions. Extensive studies on the effect of inspection and repair on the reliability of structures can be found in [9–11]. The application of the FM-based bi-linear crack growth law has been introduced for fatigue analysis [12], which reduces the excessive conservatism believed to be implicit in the single slope Paris' law approach.

Nowadays, structural design and analysis are based on probabilistic- rather than deterministic-based methods, since the former can account for the uncertainties in the loads and the models that relate them. A key driver of design is the fact that a structure is expected to perform satisfactorily within its design life [21]. For an OWT, this means that the OWT structure must fulfil its function reliably, and hence, must not become unsafe, in general, over 25 years [13]. Several studies [10,14–20] have already applied the probabilistic-based structural reliability methods for the assessment of offshore structures. However, most studies assume that the system is time-invariant. In the reality, the system is actually time-variant due to the degradation brought by corrosion and fatigue as well as time-varying loads [21].

Models used in determining the response of OWT foundations could be classified into either the one-dimensional (1-D) beam models or three-dimensional (3-D) finite element analysis (FEA) models. The 3-D FEA models are preferable because they are able to simulate detailed stress distributions and accurately capture structural responses. Owing to their high fidelity the 3-D FEA models have been applied extensively to simulate wind turbine structures [16–18,21–27], and hence, this study, will employ the FEA approach to model the responses of the jacket foundations for OWTs [21].

It is important to take into account soil-pile interactions so as to adequately capture the structural response because OWT jacket support structures are anchored via piles to the soil system. A simple approach in performing soil modelling is to use the p-y method, which assumes the stiffness of the soil are represented by equivalent springs [28]. However, a drawback of this method is that it underestimates the deflection and the modal frequency. Defining 3-D FEA brick elements is a more reliable way to perform soil modelling as this gives more accurate results [29,30]. Due to its high fidelity, the 3-D finite element analysis with brick elements is employed in modelling the soil system in this study [21].

The problem of optimising the CAPEX (capital expenditure) to OPEX (operating expenditure) ratio is an issue of priority for the offshore wind industry, and hence any cost reduction activities need to ensure safety and serviceability performance [17]. By gathering and interpreting information from complex structures, it becomes possible to assess safety levels through probabilistic approaches, optimising maintenance strategies and facilitating planning for critical repairs and retrofits. Advanced monitoring systems are now available at a lower cost, allowing the collection of loading and loading effects as well as structural response data. SHM and CM systems are designed to monitor such information over a relatively long service period in order to distinguish anomalies, detect degradation and identify damage [17,31].

Artificial neural networks (ANNs) are now extensively used within the field of Structural Reliability Assessment (SRA), as noted by several studies [32–35], owing to their universal function approximator property. In ANNs, the relationship between input and output variables is established during an iterative training process to facilitate the prediction of outputs given any input. According to [32], the most widely used ANN architecture is multi-layer feedforward network. ANNs can predict highly nonlinear functions over the entire domain accurately [34]. Previous studies have already used the response surface method based on ANN [35] since it is more efficient compared with traditional response surface methods for reliability assessment. In [32], it is claimed that this is especially true for complex structures, as long as appropriate feature selection techniques are employed [21,35].

Ziegler and Muskulus [36], analysed crack growth on a Y-joint with simulations of structural response to aero- and hydrodynamic loading and Paris' law for crack propagation. Several sources applied fatigue reliability assessment methods for the design of offshore structures (i.e. in environments characterised by highly stochastic loads and resistance properties, thus necessitating the need for SRA to account for such uncertainties systematically) some of which include [7,8,10,11,16–18,20,21,26–28,37,37–39]. In [15], the fatigue reliability of fixed offshore platforms was investigated by analysing different failure scenarios. The Palmgren-Miner's rule and S-N curve were employed to estimate the accumulated fatigue damages in the limit state function (LSF). In [38], the fatigue life of welded tubular joints are estimated by using spectral fatigue damage approach. An LSF defined based on the Dirlik probability density function, and the S-N curve approach was developed. In [37] low cycle fatigue and crack growth reliability assessment of an OWT foundation during its design life was performed. The analysis included different loading scenarios, and uncertainties such as those related to geometric properties, defects, among others were taken into account in the study. In [40], investigations conducted based on a reliability-based method to assess the structural integrity of offshore tubular joints were performed.

According to [9], to accurately evaluate the effect of an inspection and repair strategy of structures subjected to degradation resulting from crack growth, application of FM models are required to describe crack propagation. The reliability methods applied to account for inherent uncertainties with respect to selecting an optimal tool for making a proper decision, which enables a balance between design criteria, and inspection and repair plans include S-N and FM formulations. In [41,42], a methodology for the calculation of fatigue reliability (FR) of universal joint in an articulated offshore tower was presented. It was reported that the S-N curve approach yields a significantly conservative approximation of POF

when compared to the FM approach. Dong et al., [10], performed the fatigue reliability of welded multi-planar tubular joints of the support structure of a fixed jacket offshore wind turbine in a water depth of 70m. The S-N and FM approaches were applied taking account of corrosion-induced crack growth rate via a general uniform corrosion model in the study [7,21].

A sub-category under this area is the damage tolerance approach for probabilistic pitting corrosion fatigue life prediction performed by [21,43] wherein comprehensive mechanistic-based probabilistic models for pitting corrosion fatigue life prediction by including all stages were presented, and the FORM was implemented with the proposed models. In [21], a generic reliability assessment framework that combines parametric FEA modelling, RSM, and reliability assessment specifically for complex nonlinear OWT jacket type support structures in the presence of highly stochastic variables, and taking into consideration, specifically, time-dependent phenomena such as fatigue as well as degradation mechanisms such as corrosion was developed. Two ANNs were trained to relate various stochastic variables for predicting the performance function. The two ANNs were employed in order to have an intermediate predictor for a stochastic variable, which is more advantageous because of the added interpretability of results. An advantage of the proposed methodology is that the first ANN architecture enabled a significant reduction in the computational cost, which would have been required to simulate global behaviour of the support structure thus allowing other global parameters to be incorporated. Other advantages of the developed non-intrusive formulation framework include adequately accounting for 3D effects whilst modelling the fatigue crack growth behaviour as this enables us to further investigate properties difficult to study experimentally, among several other advantages. This has been previously developed by the authors and will stand as the basis for the present study.

This paper aims to assess for the first time various fatigue reliability formulations using either S-N or FM approaches focusing on the FM bi-linear crack growth law, with a view to compare their degree of conservativeness and application range. Fatigue reliability analysis (FRA) of a typical tubular OWT was carried out, whose jacket support structure is designed for a site with a water depth of 50 m. In the bilinear FM method, it is assumed that both segments of the crack growth law are either correlated or uncorrelated in the calculation of the reliability index (RI). An advanced reliability assessment of OWT jacket foundations is proposed through a combination of reliability analysis methods and assumed SHM/CM technology. A 3D stochastic parametric FEA model of OWT jacket foundations is developed, incorporating the effect of soil-structure interactions. A series of stochastic FEA simulations of the OWT support structure is carried out, taking account of stochastic variables, such as wind loads, wave loads and soil properties. ANN-based response surface methodology (ANN-RSM) is then used to post-process the FEA results so that the performance functions are now expressed in terms of the relevant stochastic variables. FORM (first-order reliability method) is then used to compute the reliability indices, evaluating the reliability of the OWT support structure in manageable computation time. Then the reliability of the structure is reassessed and updated, in the presence of assumed SHM/CM data. Apart from enhanced accuracy, the updated reliability index will provide valuable information regarding making decisions pertaining to the inspection and maintenance of the structure.

Part of this work involves investigating the fatigue reliability of the jacket reference support structure due to wind and wave loads as well as soil-structure interaction during the in-service life in the presence of assumed SHM/CM technology data. It presents estimates of the effects of other important random parameters on the reliability index by sensitivity studies. This is necessary in order to aid in the decision-making process to achieve an optimal balance of the different safety measures via performing design and planning for IMR at the design stage. A failure-critical hot-spot location where the most cumulative fatigue damage takes place is selected for use in the FRA.

The remaining parts of this paper are structured as follows. Section 2 presents a review of related literature; Section 3 presents the basics of fatigue and fracture reliability assessments; Section 4 presents the application of the methodology in a case study; Section 5 presents the results and discussion, followed by the conclusion in Section 6.

2   Basics of fatigue and fracture reliability assessment

The basic failure probability in fatigue and fracture assessment may be defined by

$$P_f = P[g(t) \leq 0] = \Phi(-\beta) \tag{1}$$

where $g(t)$ is the limit state function (LSF) and β is the safety index. The case study investigated in the upcoming sections is expressed in terms of the reliability index (RI). Φ is the standard normal distribution function [44]. Probabilities of failure implied by Eq. (1) may be approximated by means of widely used methods such as first-order reliability method (FORM), second-order reliability method (SORM) and Monte-Carlo simulation (MCS) techniques [9,44].

The FORM method incorporates a number of uncorrelated standard normal random variables. The original variables, which may, in general, be correlated and non-normal, are transformed to the u-space using well-established transformations such as the Rosenblatt's transformation. The exact failure probability is the integral of the joint probability density function over the failure domain $g(u) < 0$. The first-order Taylor series expansion of the limit state surface $g(u) = 0$ is applied at the point with the shortest distance from the origin in the u-space. An RI, β can be referred to as the shortest distance from the origin to the limit state surface in this space. The point of which the distance from the origin is minimum to the limit-state surface denotes the worst combination of random variables and is thus called the design point or most probable failure point (MPP). The calculation of the RI then becomes an optimisation problem in locating the MPP on the limit-state surface. The Rackwitz-Fiessler algorithm can be employed in recursively searching for the MPP [44–46]. After computing the RI, β, the first-order approximation to the probability of failure can be determined by using the RHS Eq. (1) [43]. This method is very simple to use, and has been found to converge quickly in most cases.

Fracture and fatigue are failure modes of note for welded offshore structures. Fatigue is a very local phenomenon, which is influenced by factors such as the local geometry, and fabrication process-induced weld defects. Crack propagation normally starts from weld defects and are driven by tensile, cyclic stresses. Cracks in jackets are restricted to the tubular joints as a result of the large stress concentration in such joints [10].

2.1   S-N curve approach

Herein, FRA was performed according to the fatigue analysis procedure described in the DNV standard [47,48]. Consequently, the thickness-corrected D curve given by DNV-OS-J101 [48] is chosen for S-N curve approach to fatigue analysis. The intercept (A) and slope (m) of the S-N curve assumed for evaluating the fatigue life of steel structure in seawater is given as 15.606 and 5, respectively.

2.2   Fracture mechanics approach

2.2.1   Fracture mechanics analysis of planar flaws

Fatigue reliability is often based on an FM approach given by the Paris' crack propagation law [9]. As set out in the BS 7910 [12], there are two methods outlined for the assessment of planar flaws both based on FM crack analysis under fatigue loading which consists of a general procedure and a simplified

procedure related to S-N curves. In these methods, the fatigue life is calculated by integrating the crack growth law. The general procedure enables the cyclic stress intensity factor expressed accurately to be employed as well as specific data for fatigue crack growth. The quality category procedure entails the use of FM calculation results which have already been carried out and presented graphically.

The FM assessment usually employs conservative estimates of the various parameters required. However, it is imperative to use an alternative approach by applying reliability methods to take into account the randomness in the parameters. It is often assumed that a flaw is a crack with a sharp tip and its propagation is governed by the law related to crack growth rate, da/dN, and stress intensity factor range, ΔK, for a material containing flaws. The crack growth law is empirical and normally depicted that a sigmoid curve cane can be used to represent the overall relationship between da/dN and ΔK in a $log(da/dN)$ versus $log(\Delta K)$ plot. It is reasonable to assume that the central portion of the plot follows a linear relationship (i.e. the Paris' law), or to represent the data by two or more straight lines to achieve greater accuracy. The crack growth rate is insignificant at low values of ΔK below the threshold stress intensity factor range, ΔK_0. There is a rapid acceleration in the crack growth rate as the maximum stress intensity factor K_{max}, at high values of ΔK tends toward the critical stress intensity factor for static load failure, K_c. However, the assumption that the central portion is applicable to all ΔK values (from ΔK_0 up to failure) is valid. The Paris' law equation is expressed as [12,49,50]:

$$\frac{da}{dN} = C(\Delta K)^m \qquad (2)$$

where C and m are material coefficients and also depend on environmental effects. For $\Delta K < \Delta K_0$, da/dN is assumed to be zero. The stress intensity factor range, ΔK, is a function of geometry, Y, stress range, $\Delta\sigma$, and instantaneous crack size, a, and is calculated from the following equation:

$$\Delta K = Y(\Delta\sigma)\sqrt{(\pi a)} \qquad (3)$$

The overall life is calculated by substituting Eq. (3) into Eq. (2) and integrating the following equation [21]:

$$\int_{a_i}^{a_f} \frac{da}{Y^m (\pi a)^{m/2}} = C(\Delta\sigma)^m N \qquad (4)$$

In BS7910 [12], the application of the bi-linear crack growth law for the fatigue assessment of welded structures is recommended. According to [9], a comprehensive data collection from several sources was carried out, and a crack growth law having two segments was recommended for steel structures. Different uncertainties in both segments of the crack growth law were reported with the (lower) near-threshold segment having the largest variability. The larger variability may be due to the proximity to the small-crack regime and hence the inherent uncertainty of the ΔK threshold whereby the material experiences no crack growth below this. In contrast, the upper segment has lower uncertainty because the crack growth rates behaviour is well inside the stable region with high values of ΔK. However, there is a lack of information on the degree of correlation between the two segments. According to [9], some studies assumed that the two crack growth law segments are uncorrelated. The effect of correlation in failure probability is investigated herein.

2.2.2   SMART© fracture

Simulations based on fracture has relied on two models: conventional cohesive zone modelling (CZM) and, of recent, the eXtended Finite Element Method (XFEM). The CZM is most appropriate for the

simulation of de-bonding of adhesively attached surfaces. The CZM is commonly applied for simulating composites, but it is not ideal for simulating the crack growth in the bulk of a material [51].

The XFEM performs better when simulating internal cracks. As packaged in the ANSYS toolkit, in the XFEM, the need for re-meshing regions near the crack tip is eliminated. Instead, an extended finite element enrichment area is defined near crack tip regions where it is most likely that the crack propagates. In the XFEM, the special volume elements in the enrichment zone are split from its centre. Hence, a finer mesh is generated by splitting existing cells rather than re-meshing. However, a drawback of the XFEM is in its inability to limit the enrichment regions as it increases, thereby making it computationally costly, and as such, the simulation becomes time-consuming. Therefore, it is difficult to scale up the XFEM to large projects, and this led to the development of the SMART$^©$ fracture tool.

The Separating Morphing and Adaptive Re-meshing Technology, SMART$^©$ relies on the Unstructured Mesh Method (UMM) process. In the SMART$^©$ as a result of automatic crack propagation at each solution step, the mesh is being updated from crack-geometry changes. This function is as packaged in the ANSYS R19 facility. Rather than applying the enrichment technique, it employs a localised re-mesh function as the crack propagates. Unlike the XFEM, an advantage of the SMART$^©$ is that it enables the simulation to be scaled up for larger projects as a result of its property of limiting the re-mesh to a small area near the crack tip at each iteration. Another advantage of this technique is that the development of new elements is not required and default/ standard elements included already in mechanical, such as the conventional solid 187, 186, etc. can still be applied. Also, the software permits designers to enter alternative crack growth laws as these emerge from new research about the particular material being modelled. Further information on the characteristics of the SMART$^©$ fracture can be found in [21].

The SMART fracture$^©$ method is applied in calculating the stress intensity factor range and crack extension. The accuracy and scientific soundness of the SMART fracture$^©$ tool was demonstrated by the same authors in other studies [7,21] using a similar purpose-developed model to that employed in the current study through a validation exercise which involved comparing the fatigue crack growth rate (FCGR) prediction of this tool with experimental data of the same test set-up, among others.

2.3 Limit state function based on the S-N curve approach

Significant cyclic loads induced by the environment are imposed on OWT jackets making their design to be driven by FLS. The FLS assessments can be performed by applying two methods, i.e. S-N curve method and FM method. According to the S-N curve method, the number of loading cycles to failure, N, can be determined from [26]:

$$log\,N = A - m\,log\,\Delta S \qquad (5)$$

where A and m are the intercept, and the slope of the S-N curve on the log-log plot, respectively, and ΔS is the stress range. Design standards, e.g. DNVGL-ST-0126, generally prescribe the intercept A and slope m. The limit state function of FRA based on the S-N curve approach can be determined from [17,52]:

$$g_{f,SN} = log\,N - log\,N_t \qquad (6)$$

where subscripts f and SN represents the FLS, and S-N curve approach, respectively; N is the number of loading cycles to failure as obtained from Eq. (5), N_t is the number of loading cycles expected during the given design life. N_t can be calculated by using rated rotor speed n_{rated} and availability η_a (98.5%) on the site selected [25,53]. Hence, assuming a design life of 24 years, the number of cycles is given as:

$$N_t = \eta_a . n_{rated} \times (24[year] \times 365[day/year] \times 24[hour/day] \\ \times 60[min/hour]) \tag{7}$$

For the calculation of the fatigue RI across the nominal service life of the asset, a quasi-static approach is assumed, where the annual reliability index can be calculated and plotted accordingly for the 24 years of consideration.

2.4 Limit state function based on fracture mechanics approach

Compared to the S-N curve method, the FM method is more detailed and involves evaluating crack growth. The failure function for fatigue as a function of time can be written as $g(t) = a_f - a(t)$. The performance function for FRA based on LEFM is given by:

$$g_{f,FM} = \int_{a_o}^{a_c} \frac{1}{Y(a)^m (\sqrt{\pi a})^m} da - C\Delta S^m (N(t) - N_o) \tag{8}$$

where subscript f and FM represents the fatigue limit state and FM approach, respectively; a_o is the initial crack depth (or the crack depth at time t_0); a_c is the critical crack depth; $Y(a)$ is the compliance function; m and C are material constants; $N(t)$ is the total number of stress cycles in the time period $[t_0, t]$; and N_o is the initial number of stress cycles.

According to [36], the FM approach is more complex than the S-N curve design, which increases the risk of gross errors. In this study, it is assumed that the errors due to the complexity of the FM approach may be reduced as a result of using the ANSYS SMART Fracture© FEA facility. Hence, in this study, owing to the high-fidelity of the FEA model, it was assumed that this has accounted for model uncertainties which may exist due to errors if analytical calculations were to be used. The Non-intrusive formulation used herein enables an enhanced analysis leading to more accurate results as it utilises the 3D simulation method as established in [21].

3 Application using a case study

3.1 Design considerations for OWT support structures

The reference case adopted for this analysis includes a baseline 10MW National Renewable Energy Laboratory, NREL wind turbine with wind speed of the site as 20 m/s, attached to an 88.4 m tower, a transition piece (TP) and is supported by a jacket foundation. The jacket is a vertical height of 66 m, and the structure is anchored by pile embedded 42 m into the soil system and submerged into 50 m deep water. The piles feature a batter angle as they are to be driven through the legs. The TP is 7 m in length and connects together the jacket and the tower [5,6]. The OWT jacket support structure was modelled in the ANSYS workbench environment, which is well-established FEA software [26]. The schematic of the jacket wind turbine is, as shown in Figure 1. See also Figure 2 and Ref. [7] for more details. In the present study, the normal operating condition of the wind turbine is considered mainly, which is also defined as the design load case, DLC 1.2 in IEC 61400-3. The wind and wave forces are simulated to always assume the same direction, and all sea states considered to be in only one direction, such that the results of the long-term fatigue loads should be conservative. This is a simplified assumption of the DLC 1.2 as outlined in IEC 61400-3.
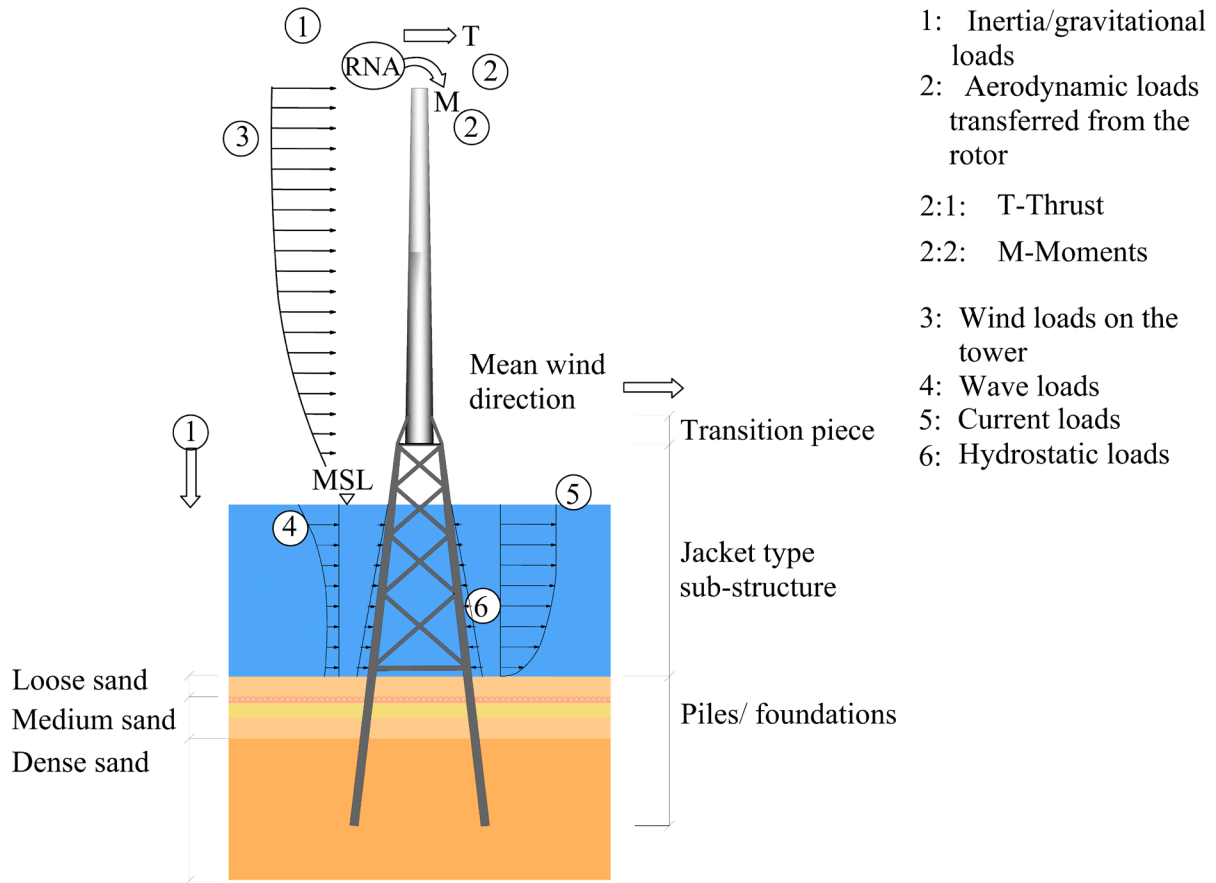
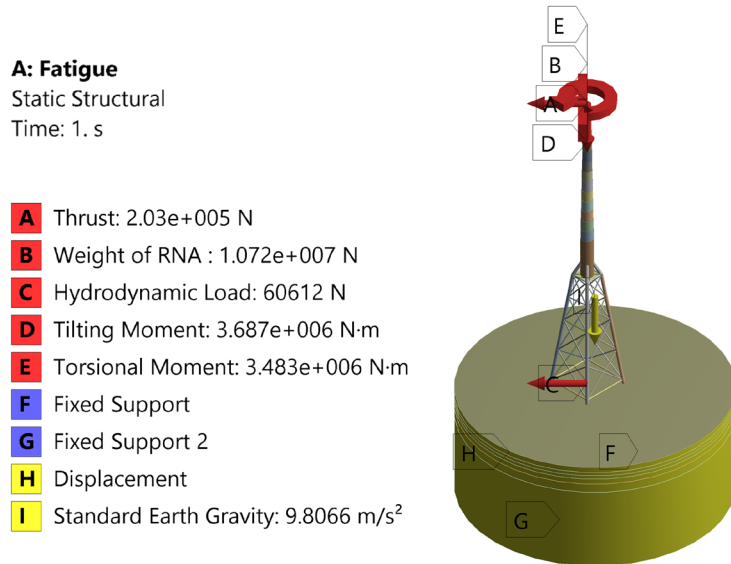*Figure 1. Representation of the loads on the support structure of the OWT and jacket geometry embedded in layered soil*

A: Fatigue
Static Structural
Time: 1. s

A	Thrust: 2.03e+005 N
B	Weight of RNA : 1.072e+007 N
C	Hydrodynamic Load: 60612 N
D	Tilting Moment: 3.687e+006 N·m
E	Torsional Moment: 3.483e+006 N·m
F	Fixed Support
G	Fixed Support 2
H	Displacement
I	Standard Earth Gravity: 9.8066 m/s²

Figure 2: The 3D structural model with applied loads and boundary conditions on a global scale (Fatigue load case)

3.1.1 Parametric modelling of OWT jacket support structures: Geometry, materials, structural components and soil profile

The tower, TP, jacket, and piles are assumed to be made of S355 steel having Young's modulus of 210 GPa, density of 8500 kg/m^3, and a Poisson's ratio of 0.3 [5,6]. Besides the OWT foundation, another design factor of note that could impact the structural response model of the pile-jacket-tower assembly is the soil-structure interaction. In order to enhance the accuracy of results calculated, the soil-structure interaction aspects are incorporated in the present study [54]. Hence, the soil profile as simulated herein is based on data which corresponds to a K-13 deepwater site located off the coast of Netherlands. Six layers of sand representing the soil profile and their corresponding parameters based on site measurements are entered into the simulation as derived from [5,21,26]. The soil system is modelled to have a cylindrical shape (D=140 m, H=50 m) consisting of six different strata in ANSYS. The Drucker-Prager Strength Linear model is assumed to describe the behaviour of the soil material [55]. This model is used to calculate the yield stress of each soil strata. The yield strength of the soil, σ_{ys}, according to the Drucker-Prager model, can be calculated from:

$$\sigma_{y,s} = \frac{6c \cos \phi}{\sqrt{3}(3 - \sin \phi)} \tag{9}$$

where, ϕ represents the angle of internal friction and the cohesion value is represented by c. The coefficient of friction between the soil and the pile, C_f can be calculated from [29].

$$C_f = \tan \left(\frac{2}{3}\phi\right) \tag{10}$$

3.1.2 Mesh sensitivity analysis

A critical step which affects the performance of an FEA is the mesh generation. The ANSYS software package provides a reliable and powerful structure mesh generator with the capability of generating a consistent mesh in the whole structure with a minimal computational requirement. A mesh sensitivity analysis was conducted for optimising the element size, thereby enhancing the precision of results. The results are presented in Table 1. Based on the mesh sensitivity analysis results, the Von-Mises (equivalent) stress converged at the soil element size of 2m and support structure element size at 0.5m, which corresponds to a total number of elements of 190,222. Similarly, the mesh convergence test was performed with respect to the RI for the developed non-intrusive method and similar results were obtained with the RI converging at the same element size as achieved in the foregoing. The display of the optimised mesh for the support structure as simulated in ANSYS is depicted in Figure 3.

Table 1: Mesh sensitivity [26]

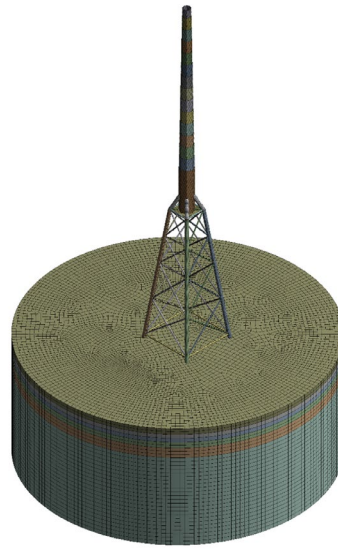| Soil element size (m)	Jacket structure element size (m)	Number of elements	Maximum Von-Mises stress (Pa)
8	2	8047	2.5297E+08
4	1	36,164	2.5328E+08
2	0.5	190,222	2.5346E+08
1	0.25	1,298,092	2.5353E+08

Figure 3. 3D display of meshing performed on the structural model [26]

3.1.3   Validation

In order to validate the structural model developed, the results of the deflection in static analysis and modal analysis for the support structure against data from the reference OWT [26]. Results of the modal analysis and deflection are depicted in Figure 4, and Figure 5 and their comparison can be seen in Table 2 and Table 3, which shows that the model approximately predicts the first eigen-frequency to the 3P frequency of the rotor. Moreover, the relative difference between the present study and as obtained from references is 0.12% as the eigen-frequency calculated is 0.21346 [6,56]. Also, the deformation at the elevation of the rotor-nacelle assembly (RNA) and the base of the tower is 1.236 m and 1.6085×10^{-1}, representing -0.46% and -3.44% relative difference between the present model and as obtained in the reference [6]. These differences are considered to be acceptable.
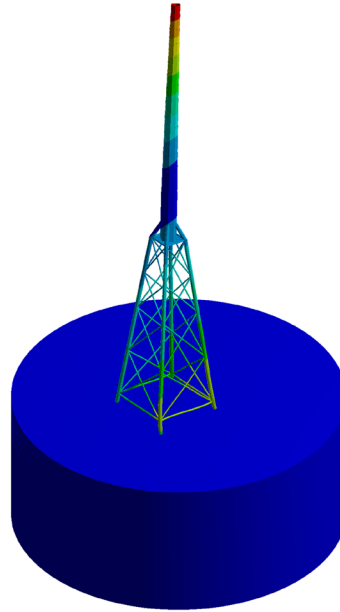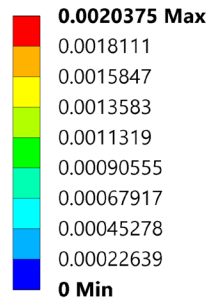
Figure 4. Display of structural model's modal analysis results showing the first mode frequency [26]
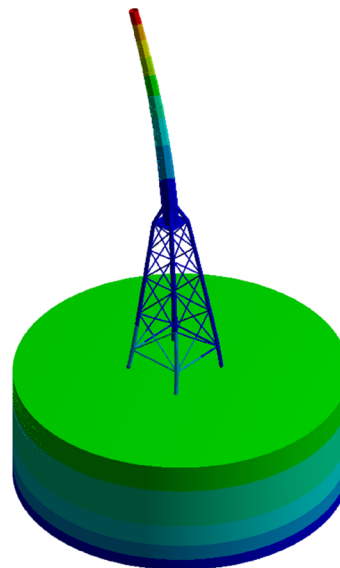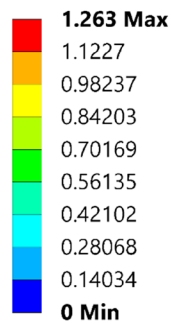

Figure 5. Display of results of total deformation showing the deflection at RNA level [26]

Table 2: Comparison of the support structure mode frequencies with reference values [26]

Mode frequencies (Hz)	Present	References [6,56]	% Difference
1st side-to-side bending	0.21346	0.21320	0.12%
1st fore-aft bending	0.22297	0.21629	2.99%
2nd side-side bending	1.1602	1.0313	11.11%
2nd fore-aft bending	1.5292	1.6561	-8.29%

Table 3: Static deformation of the baseline 10 MW wind turbine jacket [26]

Load case	Displacement at RNA			Displacement at the tower base		
	Present	Ref. [6]	% Diff	Present	Ref. [6]	% Diff
Mass/ Thrust						
RNA/ 3.4 MN	1.263 m	1.2688	-0.46%	1.6085×10^{-1}	1.6639×10^{-1}	-3.44%

3.1.4 Calculation of loads on OWT support structures

In the present study, the normal operating conditions are assumed to represent the environmental conditions for the FLS design approach adopted. The wind, wave, and current loads are manually calculated and then entered in the parametric FEA model.

According to the IEC 61400-1 [57], the normal wind climate conditions assumed in the present study are considered to be cyclic structural loading conditions and are calculated as thus:

$$V(h) = V_{ref} \frac{\ln\left(\frac{h}{z_0}\right)}{\ln\left(\frac{h_{ref}}{z_0}\right)} \tag{11}$$

where z_0 is the roughness coefficient (see [48]). After generating the wind speed profile, the horizontal load exerted on the tower, TP and nacelle can be expressed as:

$$F_x = \frac{1}{2} C_D \rho_e (V_{max})^2 A \cos \alpha \tag{12}$$

where C_D is the cylindrical drag coefficient (for the tower and TP) and plate drag coefficient (for the nacelle), A is the area being pushed by the wind, and α is the inclination angle of the wind with the horizontal axis. The effects of the blades are not taken into account in this study.

Morrison's equation is employed in the calculation of the wave forces. The equation is constituted of the drag and inertia terms, where the drag identified by the drag coefficient C_d, and the inertia identified by the inertia coefficient C_m [58]. Morrison's equation can be expressed as:

$$F = F_d + F_m = \frac{1}{2} \rho_w C_d D |u_x| u_x + \rho_w C_m \frac{\pi D^2}{4} \frac{dU}{dt} \tag{13}$$

where U is the undisturbed fluid velocity, $\frac{dU}{dt}$ is the acceleration of the fluid, ρ_w is the water density, and D is the diameter of the cylinder. The wave profile data such as water levels and wave data of interest for the K-13 deepwater site derived from [7] was used in the current study. In terms of the structural integrity, environmental loads, such as the tidal currents and wind-driven currents, are not significant threats in shallow-water circumstances. However, these can contribute to other significant excitations such as those generated by the wind and waves. The tidal current profile at distance z from still water level can be denoted by the current speed $(v(z))$. The current speed variation from the current at the still water level v_0 through the distance to the topwater column can be described exponentially. This is expressed as:

$$v(z) = v_0 \left(\frac{h + z}{h}\right)^{\frac{1}{7}} \; for \; z \geq 0 \tag{14}$$

where h is the water depth. The extreme tidal current is assumed to occur at approximately the mean water level, with zero tidal currents at high and low tide. Having obtained the tidal current profile, the assumption of a constant over depth current will be made. Wind-driven currents occur due to the action

of shear forces on the water surface resulting from wind and thus, are likely to act in a similar direction with the wind. According to IEC61400-3, the sea surface wind-driven current can be estimated from:

$$U_{wind} \approx 0.01 U_{1h,10min} \tag{15}$$

where $U_{1h,10min}$ is the hourly mean at 10m height.

The submerged parts of the jacket are subjected to a water column pressure referred to as the hydrostatic pressure. This can be calculated via a control volume analysis of an infinitesimally small cube of fluid, assuming a constant gravity and density through depth. Hence,

$$p(z) - p(z_0) = \frac{1}{A} \int_{z_0}^{z} dz' \iint^{\rho}(z')g(z')dA = \int_{z_0}^{z} dz' \rho(z')g(z') = \rho g h \tag{16}$$

where $p(z)$ is the pressure at a given height z, $p(z_0)$ is the pressure at z_0, which is the top of the water column, Therefore, $p(z_0) = P_{atm}$, ρ is the water density (kg/m^3), g is gravity (m/s^2), $h = (z - z_0)$ is the liquid column height measured from the test volume to the zero reference point of pressure.

The rotor and nacelle are assumed to be concentrated or distributed masses as modelled in the FEA. Hence, the hub and blades are excluded from the parametric model. According to [54], modelling the blades will not be necessary since, besides the added mass acting on the tower top, the parked and feathered blades do not have a significant effect on the eigen-frequency of OWTs. The weight of the Rotor Nacelle Assembly (RNA) is assumed to be 10516 kN. A single horizontal axis wind turbine sustained by a jacket substructure is assumed in the present paper. Hence, this study does not cover wake effects associated with wind farm sites. Effective turbulence models are crucial in considering wake effects on fatigue reliability of OWT components in wind farms. More details on this can be found in [59]. A well-suited option to capture the most important nonlinear contributions from the blades, generators, etc. is the use of aero-servo-elastic codes such as GH BLADED, openFAST, FLEX5 and HAWC2. This is expected to produce more accurate fatigue reliability estimation but may be achieved at the expense of high computational requirements [60].

The widely used standard, DNV-OS-J101 prescribes guidelines to assess the structural integrity of OWT support structures. As set-out therein, during design, OWT support structures should be checked against four limit states FLS, Ultimate Limit States (ULS), Serviceability Limit State (SLS), and Accidental Limit State (ALS). According to several sources, fatigue is the design driving criteria for most components of OWTs, and this study will focus on the FLS [10,16]. Further description of limit state design can be found in [3, 6, 18, 50].

3.2   OWT support structure having flaws and subjected to fatigue

3.2.1   Parametric FEA

In this subsection, a parametric FEA model of the three-dimensional space frame, tower and pile assembly (as shown in Figure 2), the jacket configuration, and the sources of loads are presented. The present study is based on analysis already carried out in [21,26]. In the upcoming sections, the FM ANN architectures are used to approximate the performance by linking the input parameters with the output, the stress range. The parametric FEA developed for this study is presented below.

Fatigue damage can be assumed to initiate from the weld toe of a critical tubular multi-planar welded joint, and a section containing the initial crack can be extracted for the stochastic parametric FEA at local scale according to Refs. [7,12,21,48]. Initial flaws/ cracks can also be assumed to initiate as a result of welding/ manufacturing imperfection. Thus, a section at this location is modelled in the form of a curved plate within which the crack is located. This is performed so as to limit computational time/cost to practical levels, among other advantages.

The FEA model developed by the authors in [26] is adopted to calculate the equivalent stress at the vicinity of the crack, and this result is assumed to be exerted on the plate (see Figure 6 and Figure 7). The Equivalent stress imposed on the plate as modelled was determined to be 58.63 MPa [21].
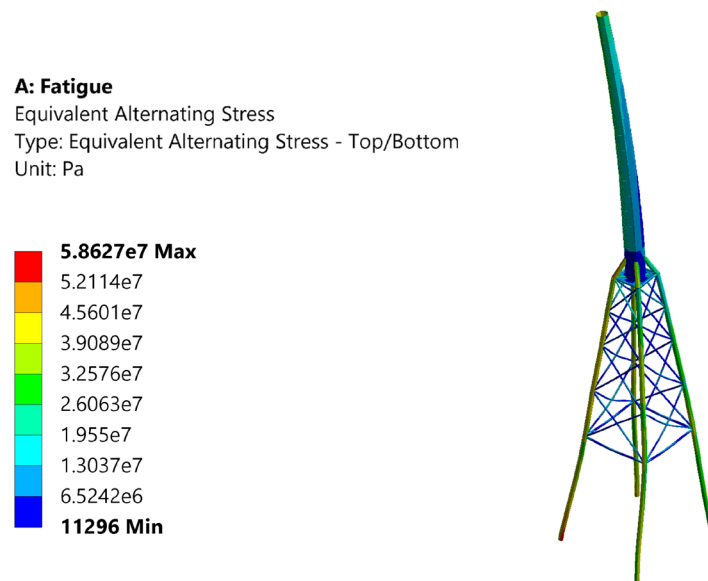

Figure 6. 3D display of structural model showing the equivalent alternating stress
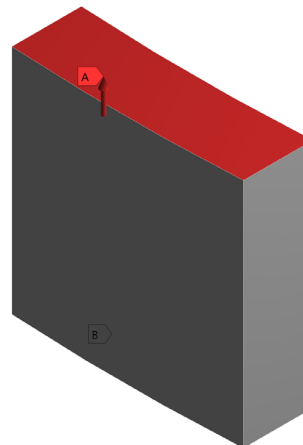
Figure 7. 3D structural model of curved plate with applied stress and boundary condiions in ANSYS [21]

3.3   Structural reliability assessment (SRA) of the OWT support structure

In this section, the SRA of the OWT support structure using first, the S-N curve approach and then second for the FM approach assuming the structure is subjected to fatigue is carried out based on the damage-tolerance approach both considering FLS as set-out in DNV-OS-J101 [48]. The fully parametric FEA model presented in Section 3.1.1 and Section 3.2.1 is employed in carrying out FEA

modelling, accounting for stochastic variables, for the S-N curve and FM approach respectively. Then all results generated are then post-processed using a developed non-intrusive formulation.

3.3.1 Stochastic variables and FEA

The stochastic variables considered in this study are presented in Table 4 for the S-N curve approach and the FM approach, assuming the bilinear FM model. Seventeen (17) stochastic variables were considered for both methods. Ten stochastic variables were considered for the first ANN, and this set-up was arrived at as described in [61]: Initially, these included the thrust force, hydrodynamic load, torsional moment, tilting moment, the weight of RNA, and three young moduli at three soil strata. The total hydrodynamic load was considered differently due to its dependence on the wave period, wave height, and current speed. To calculate the peak hydrodynamic force acting on the system the significant wave height and the current speed were assumed to follow a Weibull distribution, while the wave period was assumed to follow a lognormal distribution [3, 59, 60]. The total hydrodynamic load was then fitted into a Weibull-equivalent distribution. Distribution fitting algorithms (such as Akaike Information Criterion, Bayesian Information Criterion and Kolmogorov-Smirnov) are often applied to determine the shape coefficients of the most suitable statistical distributions, in the presence of observed data [18]. In the present study, the wind speed, significant wave height, wave period, and the current speed are reintroduced into the stochastic model and the equations incorporated in the LSF model of the FORM on implementation of the SRA.

Table 4: Stochastic variables.

Description	Mean values	Coefficient of variation (COV)	Distribution types	Reference
Young's modulus of steel [2] (GPa)	210	0.1	Normal	[18]
The major radius of initial semi-elliptical crack[2] (mm)	0.22	1	Exponential	[10,37]
The minor radius of initial semi-elliptical crack[2] (mm)	0.11	1	Exponential	[10,37]
Wind speed, V [1] (m/s)	20	0.05	Weibull	[5,56,64]
Tilting moment, M_{Tilt} [1] (kN.m)	3687	0.1	Normal	[16,21,26,63]
Torsional moment, $M_{Torsion}$[1] (kN.m)	3483	0.1	Normal	[16,21,26,63]
Maximum small crack size (mm)	0.276	1	Exponential	[10,37]
LnC_1	-29.11	1.69	Normal	[9,10,37,65]
LnC_2	-19.27	0.6	Normal	[9,10,37,65]
m_1	4.6	-	Fixed	[9,10,37,65]
m_2	1.64	-	Fixed	[9,10,37,65]
Thickness/ final crack depth (mm)	30	0.1	Exponential	[10,37]
Significant wave height, H_s [1] (m)	9.4	0.065	Weibull	[5,56,64,66]

Peak wave period, T [1] (s)	14	0.038	Lognormal	[5,56,64]
Current speed, U [1] (m/s)	1.2	0.1	Weibull	[5,56,64]
Young's modulus of soil stratum 1, E_{s1} [1] (MPa)	30	0.1		
Young's modulus of soil stratum 2, E_{s2} [1] (MPa)	50	0.1	Normal	[16,21,26,63]
Young's modulus of soil stratum 3, E_{s3} [1] (MPa)	80	0.1		
RNA Weight, W_{RNA} [1] (kg)	1,072,000	0.025		

[1]Inputs to the first ANN architecture

[2]Inputs to the second ANN architecture

For both cases (i.e. assuming the S-N curve and FM approaches), after determining which variables are to be designated stochastic, a series of stochastic parametric FEA modelling of the OWT foundation was carried out adopting the FEA model developed in Section 3 using the Design of Experiments (DoE) function as packaged in ANSYS DesignXplorer. This enables the various input parameters to be designated as stochastic with each assuming different distributions. DoE allows the generation of output parameter corresponding to the different design points as they are being varied.

3.3.2 Non-intrusive formulation

For both approaches, having defined the stochastic parameters, the performance function (PF) is determined. For example, for the FM approach, the PF is determined by substituting the small crack regime life and long crack regime life into the FLS Equation as established in [21]. The resulting safety margin can be calculated from Eq. (17). The frequency is fixed at 0.21 Hz as derived from Ref. [5]. Subsequently, the FORM is applied in estimating the fatigue reliability index.

$$g_{f,FM} = \int_{a_i}^{a_{tr}} \frac{1}{Y(a)^{m_s}\left(\sqrt{\pi a}\right)^{m_s}} da + \int_{a_{tr}}^{a_f} \frac{1}{Y(a)^{m_l}\left(\sqrt{\pi a}\right)^{m_l}} da \\ - C_s \Delta S^{m_s} N(t_s) - C_l \Delta S^{m_l}(N(t_l) - N_0) \tag{17}$$

Figure 8 depicts a flow chart of the developed non-intrusive formulation for the FM approach used herein. The algorithm begins by defining the system, the FLS and the stochastic variables in the analysis. Next, a series of FEA simulations in ANSYS is executed by varying the inputs and recording the outputs corresponding to the limit state. The FEA simulations are varied using the ANSYS DoE package via the Latin Hypercube Sampling technique. Theoretical details of ANSYS DesignXplorer© can be found in Ref. [26,67,68]. In this study, the generated data sets from ANSYS are then used to train artificial neural networks (ANN) in order to map the structural response over the domain of stochastic variables. Finally, the RI is calculated using the FORM, which has been entirely implemented by the authors in MATLAB. The steps detailed in the foregoing should be followed in a recursive process calculating the annual reliabilities and hence the reliability for different time periods can be quantified in a quasi-static way. The iterative FORM algorithm has been validated against the MCS in previous studies [21,26]. The well-established FORM is used as it offers a good balance between efficiency and accuracy for realistic problems. One limitation of the MCS method is that many simulations are required to calculate the very low values of failure probability, which is a characteristic of complex offshore structures [26]. Considering the time required, the stochastic parametric FEA simulation runs for about 5 minutes on a high-performance computer while the ANN-based RSM and FORM runs instantly.
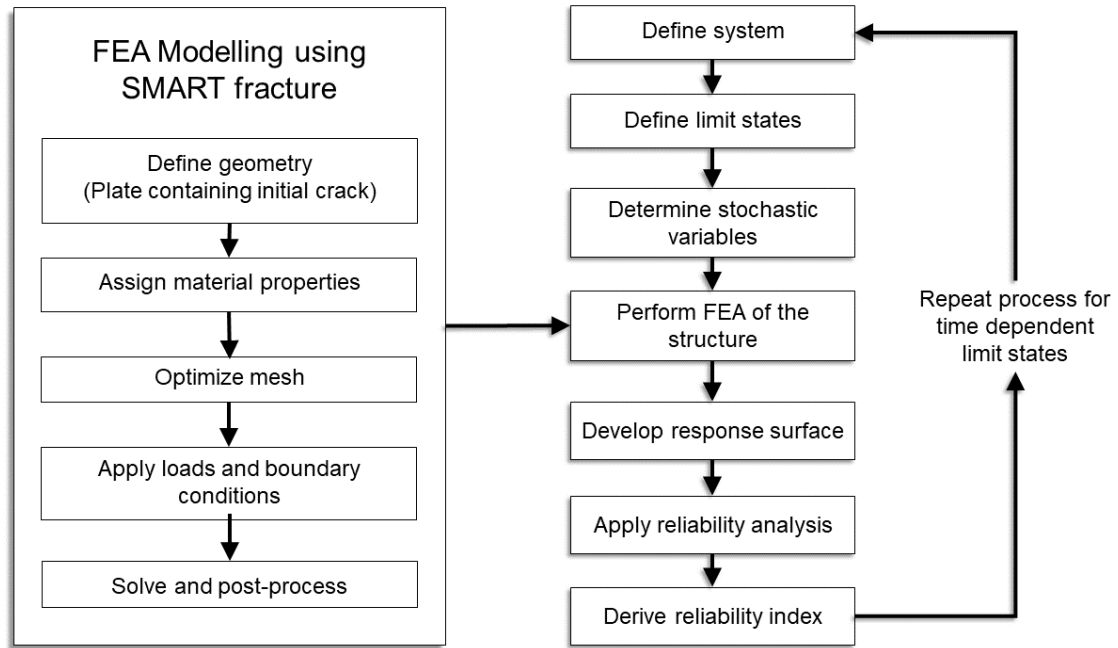
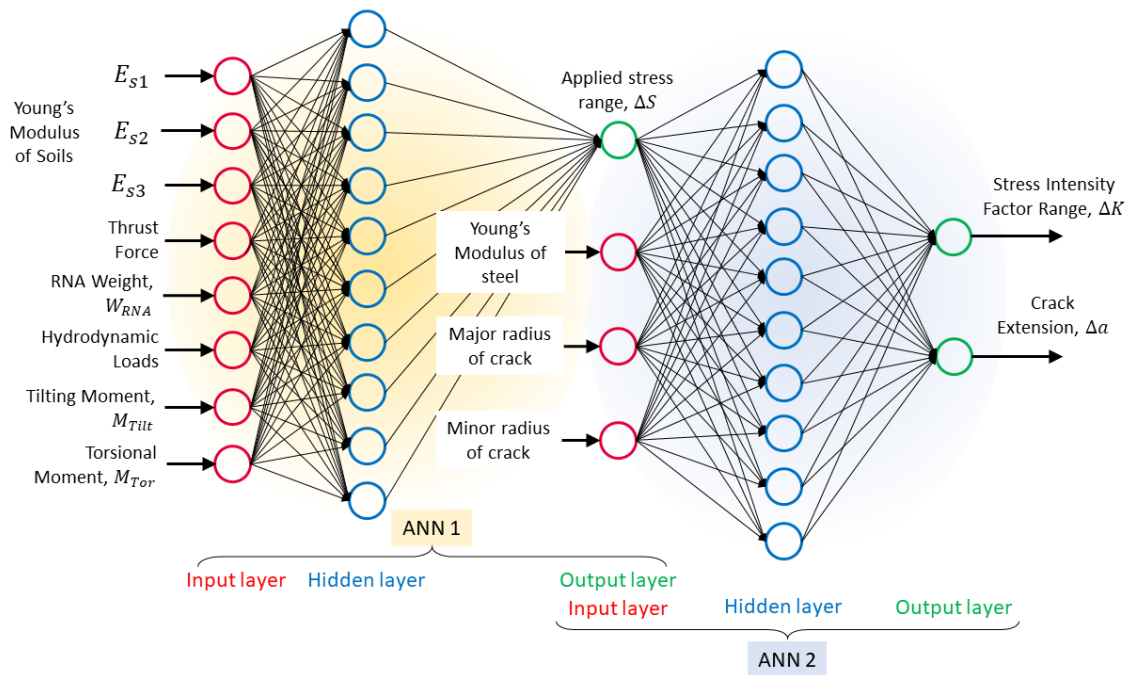*Figure 8. Flow chart of non-intrusive formulation for the FM approach* [21].

Figure 9. Two artificial neural networks (ANNs) that relate the variables given in Table 4 [21].

We now give further details to the ANN-based RSM, as follows. Two ANNs are used to predict the performance function using the stochastic variables as input. As shown in Figure 9, the first ANN aims to predict the applied stress range, while the second ANN aims to predict the stress intensity factor range and the crack extension. The architecture, the training, and testing results of these ANNs are the same as those provided in Ref. [21]. The results for training these ANNs reported high accuracy with the R-square value of more than 99% during both training and testing. This means that the trained ANNs match well with the FEA results indicating its success, and hence, are reliable predictors of the target

variables for subsequent structural reliability analysis. The readers may refer to Table 4 for a summary of the variables involved. Having obtained the performance function from the ANN, the FORM is used to calculate the reliability index β using the HL-RF algorithm developed by the authors as described in [21,26,61].

4   Results and discussion

From the fatigue reliability index curve for the S-N curve method, it can be observed that the structure maintains a reliability index exceeding the defined threshold of target reliability as specified by DNV for the nominal 24 years of operation of the structure as shown in Figure 10. When the fatigue reliability over time is estimated, the inspection activities then need to be scheduled. In order to determine the times for IMR, a reliability index threshold for the inspection need to be identified. According to DNVGL standard [30], the target reliability index of OWT support structures is 3.71. Therefore, 3.71 is taken as the reliability index threshold in this study.
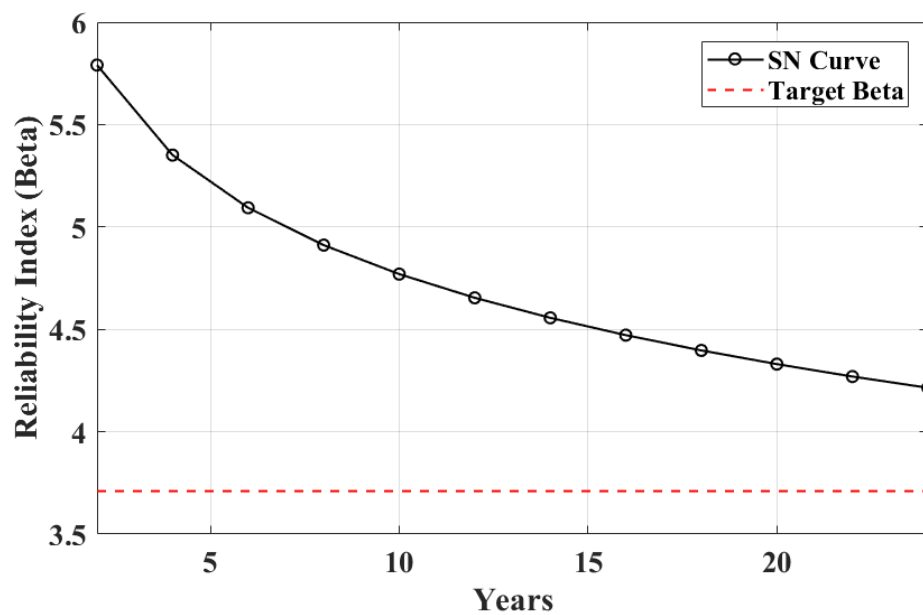
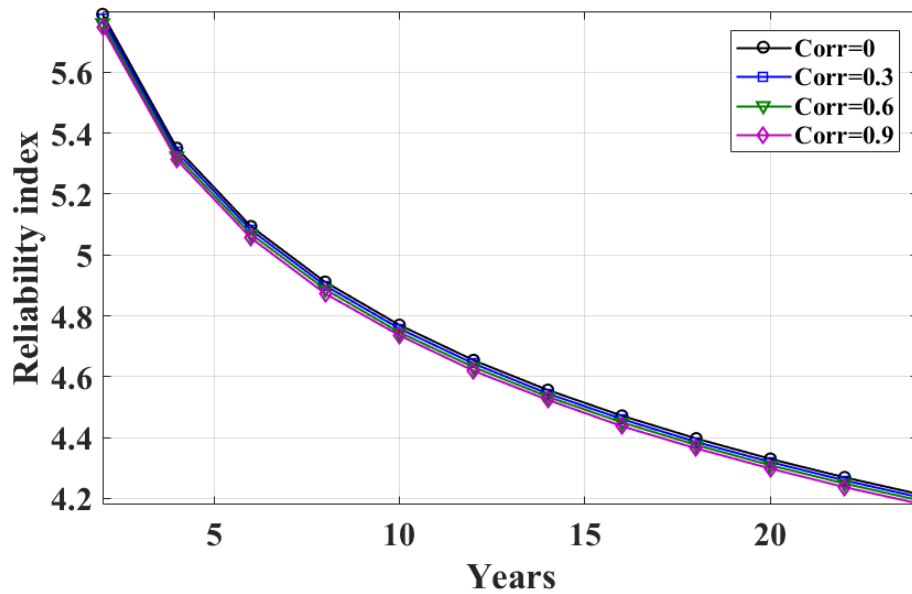*Figure 10. Fatigue reliability assessment using the S-N curve approach*

Figure 11. Fatigue reliability analysis assuming different levels of correlation between stochastic variables

4.1 Fatigue SRA results

A study is performed using the S-N curve method to examine the correlation effects of random variables on the reliability of the structure. The variables considered correlated are the wind speed and aerodynamic effects, then the wind speed, significant wave height, and wave period, and then the different Young moduli of the soils, simultaneously. The estimated reliability indices as they vary with the variation in correlation is depicted in Figure 11. As can be inferred from the figure, as the correlation between the stochastic parameters increases the reliability indices calculated decreases. Hence, this implies a negative correlation and the RI is sensitive to the percentage correlation.

Fatigue reliability assessment was carried out employing the FM modelling approach, and the results are presented in Figure 12. It can be inferred that the structure failed the defined criteria after the year 9.65 as the reliability index β will fall below the defined threshold value of $\beta = 3.71$ [16–18,63].

4.2 Comparison between the S-N curve and FM approaches

From Figure 13, it can be observed that at year 2 in the S-N curve approach, the $\beta = 5.79$ while in the FM-approach $\beta = 8.15$. Also, it can be seen that both curves intersect at year 7.05 when $\beta = 5$ whereas, at year 24 for the S-N curve approach, $\beta = 4.21$ while for the FM approach, $\beta = 1.24$. Hence, the structural reliability prediction produced following the S-N curve method gave conservative results compared to that produced using the FM approach at the start of the service life of the structure, but towards the end of the design life, the results may be overly optimistic. From the foregoing, we can establish that in terms of safety, it is better to apply the FM approach in the subsequent fatigue reliability assessments presented in the upcoming sections.

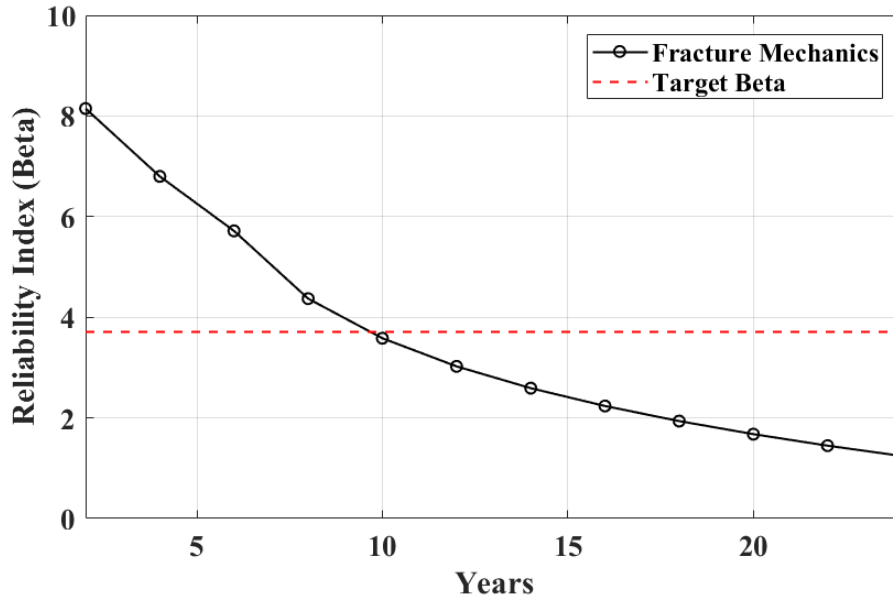*Figure 12. Fatigue reliability assessment using the FM approach*
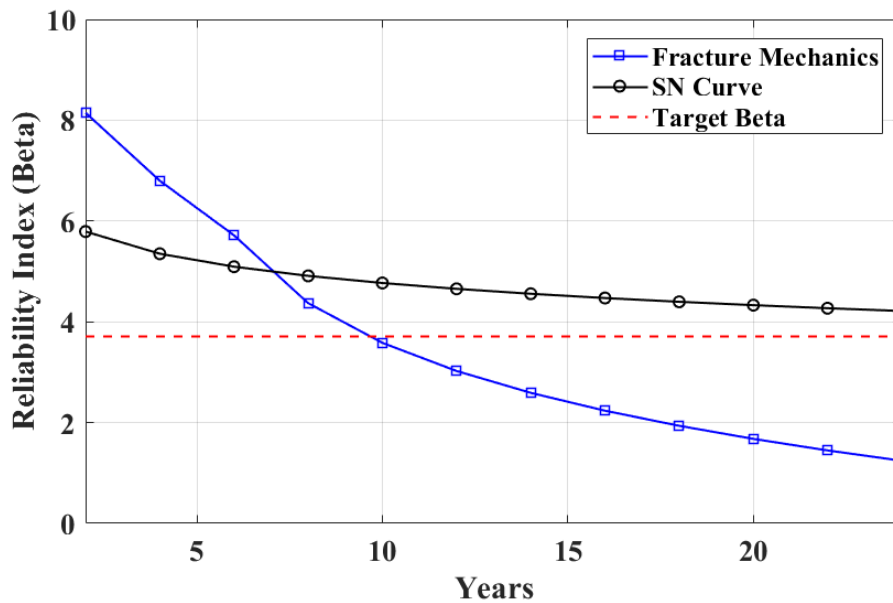

Figure 13. Comparison between the S-N curve and FM approaches

4.3   Sensitivity studies

The results of a sensitivity analysis to the fatigue reliability performed on the structure by varying different parameters is depicted in Figure 14 to Figure 21. This depicts the most critical FM parameters that have a drastic impact on the response and reliability performance of the support structure. According to [9], apart from uncertainties in the Paris' law parameter C, other parameters of note of which their uncertainties often have significant impact on the fatigue reliability of welded components include the uncertainties in the crack initiation period, the initial crack size as well as in the crack aspect ratio development. It is argued therein, however, that due to the large number of microscopical defects introduced whilst the welding process as well as the stress raising effect of the geometry of

the weld itself, the initiation time in welded structures is relatively small (10–15% of the total fatigue life). Hence, the initiation time is neglected herein, which is also a conservative assumption. In addition, it is assumed that corrosion-fatigue mechanism takes place, according to several studies [21,65,69–73].

According to the data provided in the BS7910 [12], the uncertainties of the crack growth law constant C which corresponds to the lower segment are larger than that of the upper segment. As a result of both the inherent uncertainty in the behavior of very small crack propagation and the difficulty of carrying out measurements of such rates in the tests, this also entails that the near-threshold crack growth rates have an impact. In addition, there is insufficient information with respect to the level of correlation which exists between both segments. This will have an impact on the RI results as calculated. The effect of correlation between C_1 and C_2 are analysed, as shown in Figure 14:

As can be observed the effect of variation in the correlation is pronounced at around years 6 and 8 of the operation of the structure. At this region of the FRA curves, the reliability index values decrease with an increase in the assumed correlation. It can be said that this may be at the small crack-to-long crack transition period. In other words, the reliability index curves diverge at the beginning (at the year 6 to be precise) and converge towards the end of the service life as the percentage correlation is increased correspondingly for the FM approach. As can also be seen from the same figure, with respect to the RI threshold based on the fatigue reliability curve having no correlation, 30% correlation, 60% correlation, and 90% correlation, the structure fails the defined criteria after the year 9.65, 9.43, 9.10, and 8.48 respectively. This indicates that correlation between the Paris' law constants assuming the bilinear FM model has a significant impact on the predicted fatigue RI.
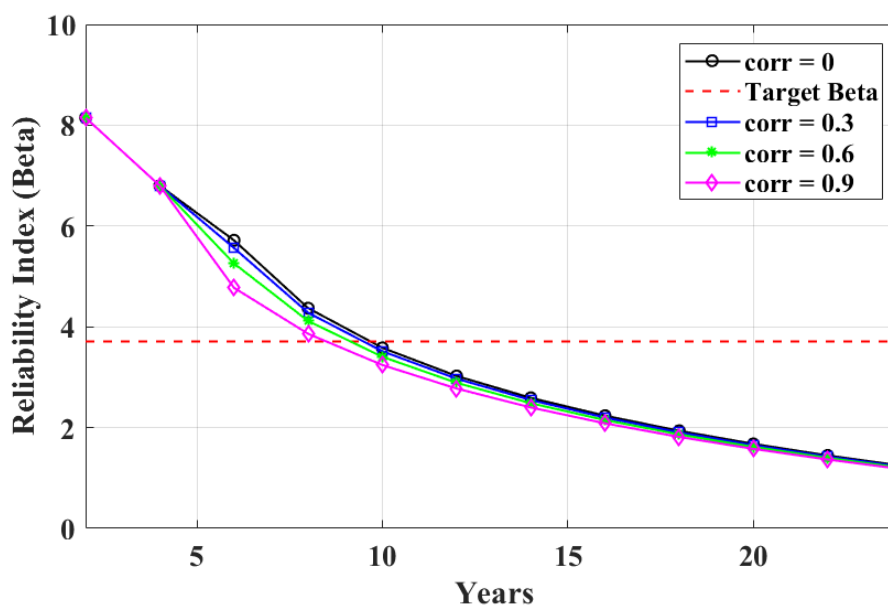

Figure 14. Fatigue reliability analysis assuming different levels of correlation between C_1 and C_2.

It is crucial to emphasise that in the context of a bilinear FM law in seawater circumstances, majority of the propagation of surface cracks is affected by the uncertainties associated with the near-threshold rate of crack growth. For through-thickness cracks, the propagation is driven by

larger crack growth rates far away from the influence of the uncertainties inherent to the knuckle of both slopes. The case study in this paper considers only surface cracks.
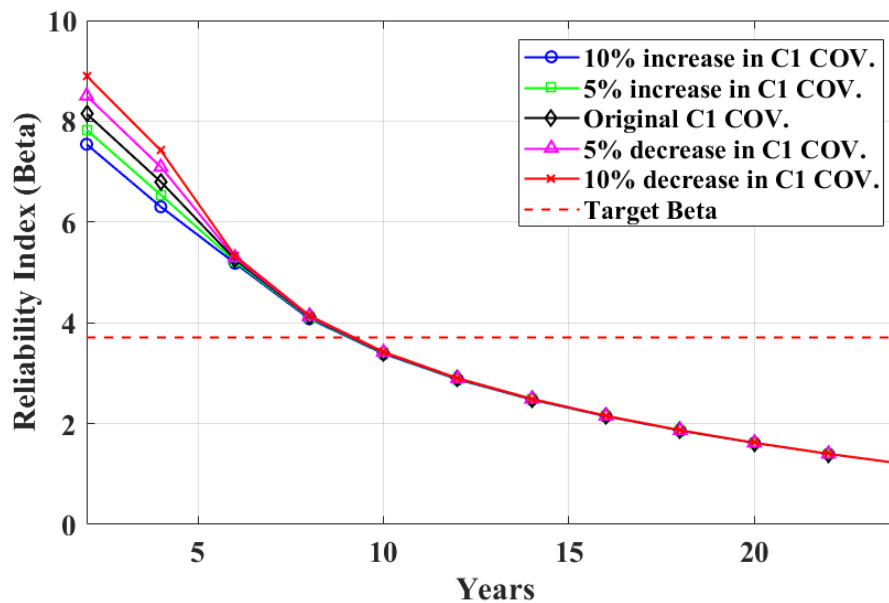

Figure 15. Fatigue reliability assessment using the bilinear FM model at different COV values of C_1

In the sensitivity studies presented in the followings, the correlated FM model is used, which is believed to represent most appropriately the bi-linear FM probabilistic formulation. In Figure 15 for the bilinear FM model, as the uncertainty measured in terms of coefficient of variation (COV) in Paris' law constant C_1 increases, there is corresponding continuous decrease in the RI magnitude initially, which converges at the 10th year. Figure 16 shows that as the uncertainty, measured in terms of COV in Paris constant C_2 increases, there is corresponding continuous decrease in the RI magnitude between years six and the year 22. As the COVs are increased there is no observed change at year 2, but the curves diverge at year four and then later converges at year 24. In Figure 17, the COVs of both terms C_1 and C_2 are increased simultaneously and it is observed that there is corresponding decrease in the RI value initially but the curves converge to the same RI at the end of the service life of the structure. Also, Figure 16 and Figure 17 depict that a change in the value of the variation coefficient affects the time to failure/ inspection time for the structure.
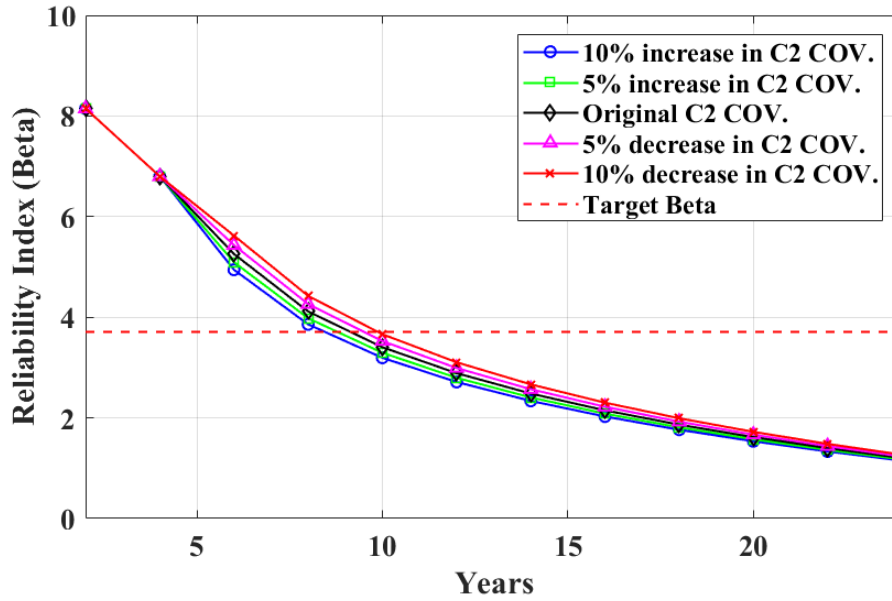
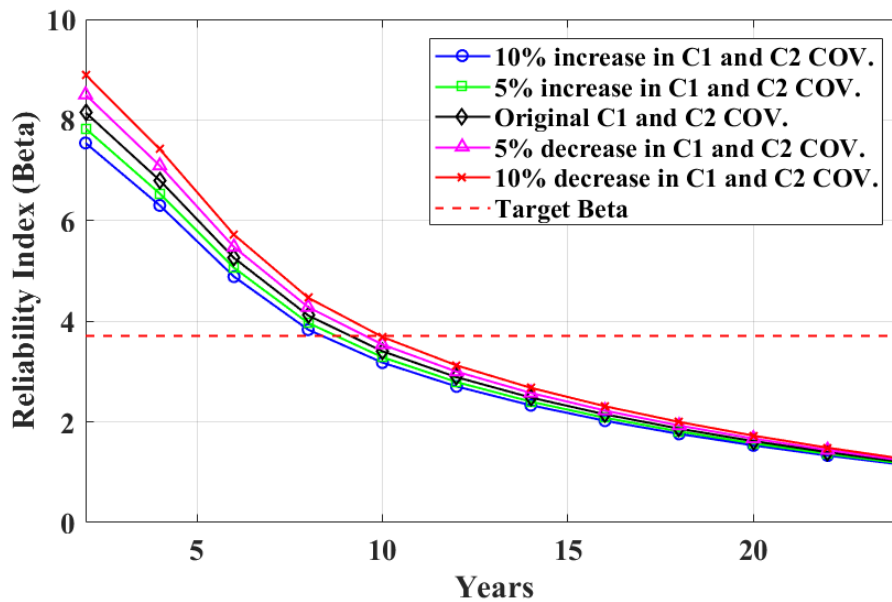*Figure 16. Fatigue reliability assessment using the bilinear FM model at different COV values of C_2*

Figure 17. Fatigue reliability assessment using the bilinear FM model at different COV values of C_1 and C_2 (assuming the COVs of C_1 and C_2 are equal)

In this study, of interest is the initial size of a surface crack in a welded joint assumed to be induced by the welding procedure itself. The initial crack size, in principle, may be referred to as the depth (or length) from which the nucleation of a flaw from surface defects has occurred and will grow under the stable crack propagation regime until a final crack size or fracture. The probabilistic sensitivity factor (α) is used to quantify the influence of the initial crack size, a_i as shown in Figure 18 and Figure 19. According to [43], these are obtained as the components of the unit gradient vector at the MPP of the limit state in the standard normal space. As can be seen in Figure 18, as the mean value of the a_i increases there is corresponding decrease in the value of the α. At the 6th year of the operation of the

structure, the curves are observed to be converging after which an increase in the value of a_i leads to slight increase in the magnitude of α. The curve finally converge in the year 10 where there is no observed change in the magnitude of α as the mean value of a_i is changed. Also, from Figure 19 a similar behavior is observed to the foregoing but this time a decrease in the COV leads to corresponding decrease in the magnitude of the α with the curves tending to converge as we are approaching the year 6. Hence, it can be inferred that the performance function by applying the FM approach is sensitive to the mean and COV of the a_i at the beginning of the service life of the structure.

These results show that it is not only the mean value of stochastic variables that control the reliability or safety of the structure, but COV also plays a significant role in determining the structure's reliability or safety. This study may prove to be efficient for optimisation and improvement of design.
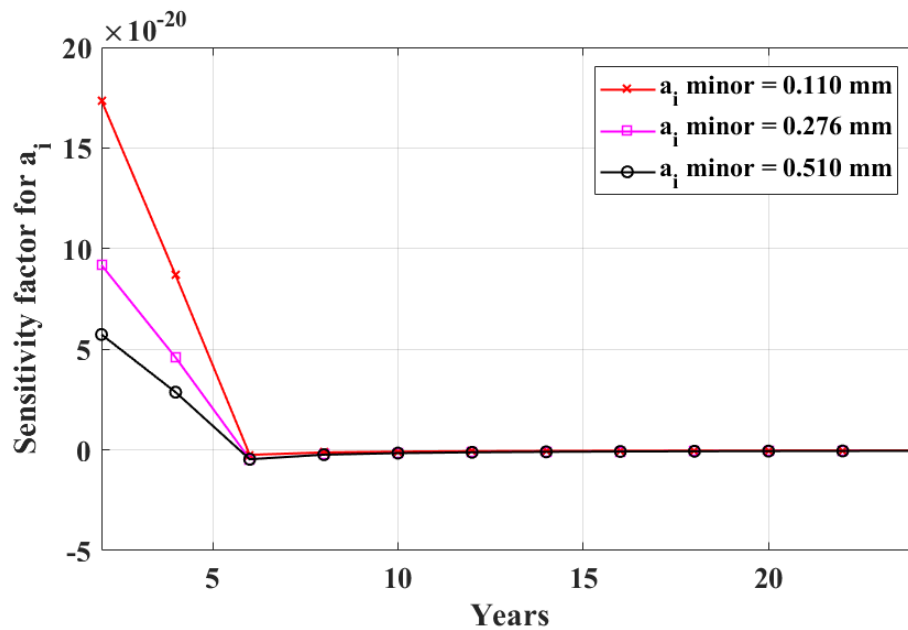

Figure 18: Variation of the sensitivity factor (α) with time at various mean values of initial crack depth (a_i).
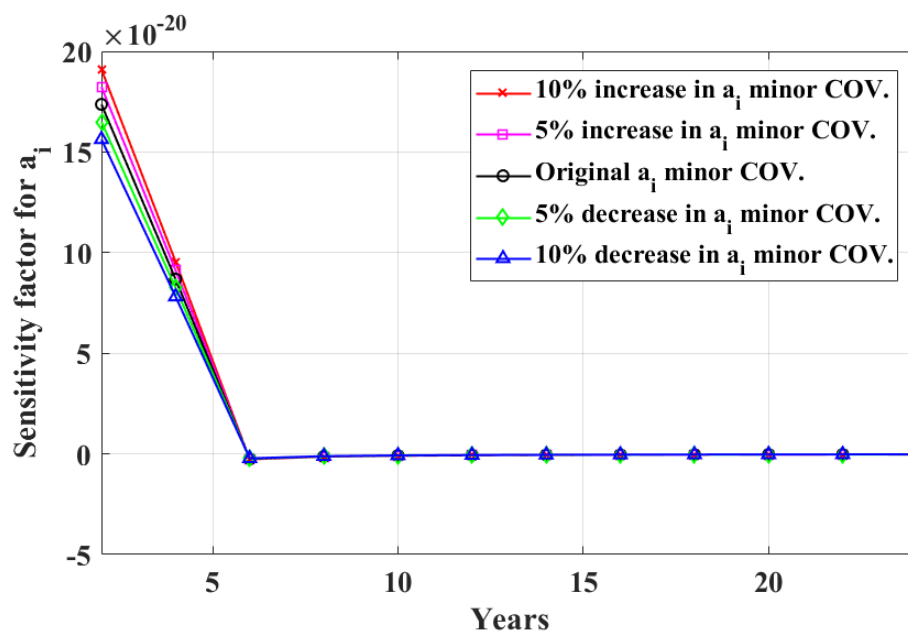

Figure 19. Variation of the sensitivity factor (α) with time at various COVs of initial crack depth (a_i).

25

4.4 Reassessment of fatigue reliability of OWT support structures in the presence of assumed SHM/CM data

During the in-service life of OWT support structures, the state of specific parameters such as crack depth and stress/strain can be measured and monitored with SHM/CM. In the presence of SHM/CM data, a reassessment of the OWT support structure's fatigue reliability can be carried out based on the FM method.

In the initial FRA, the stress range employed in the FM approach was calculated via FEA modelling. The stress/ strain history at the critical location can be measured and monitored during the in-service life of OWTs with SHM/CM systems, and these measured data can be applied in updating the fatigue stress range. For example, assuming after six years of operation, the measured fatigue stress range is 10% or 20% higher than the original values calculated via FEA modelling. Then, the OWT support structure's fatigue reliability can be reassessed based on the measured stress values and the FM method. Let case (a) denote the originally calculated fatigue stress range case and (b) and (c) represent the cases with 10% and 20% higher measured values than the original, respectively. For instance, Figure 20 shows the original and updated reliability index over time. As can be inferred, the updated reliability index curve in the case (b), was lower than the case (a). Thus, a negative correlation is observed as a higher value of stress range yields lower reliability.

After the fatigue reliability overtime is calculated, it is necessary to schedule the inspection activities. In order to estimate the times for inspections, a threshold RI for the IMR needs to be identified. The target/ threshold RI value is taken to be 3.71, according to [30,63]. As can be observed from the same figure, the inspection based on the original reliability curve (case (a)), and updated reliability curve for cases (b) and (c) are 9.2, 9.08, and 8.75 years, respectively.
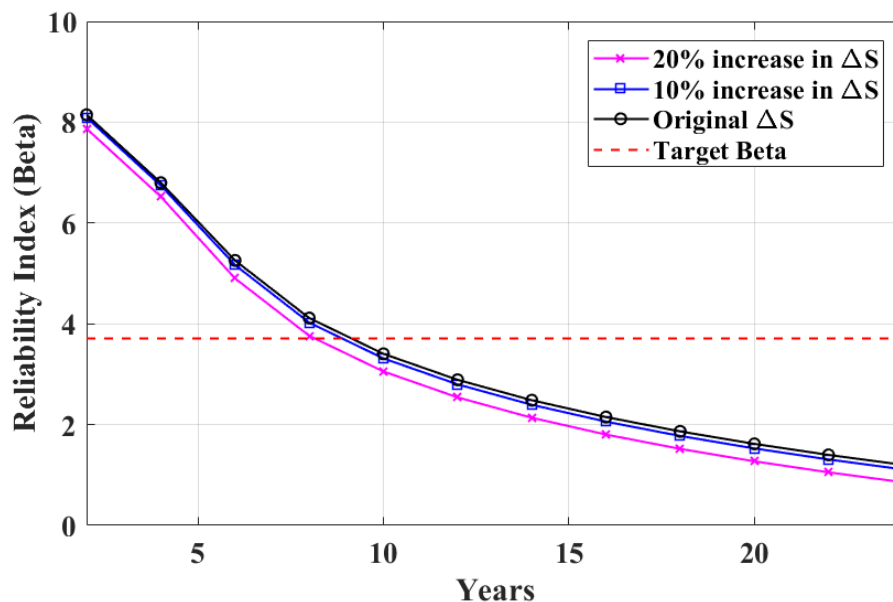

Figure 20. Fatigue reliability assessment using the FM approach at different values of the stress range
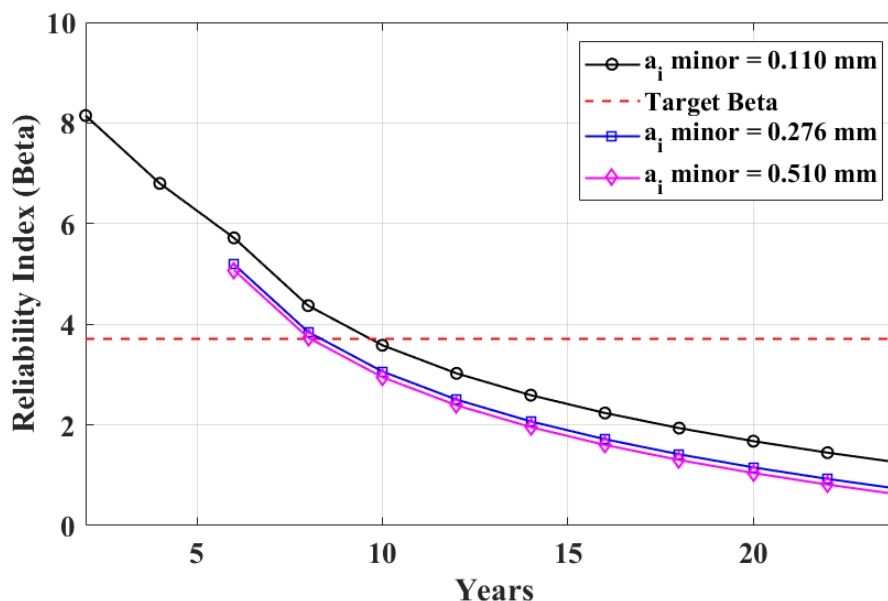
Figure 21. Fatigue reliability assessment at different values of initial crack size

The FM FRA method is dependent on the assumed initial crack depth. The measured crack depth via SHM/CM system during the in-service life of OWTs can be used in updating the calculated RI based on the FM approach. Figure 21 depicts such an example wherein the initial crack depth is assumed to be 0.11mm. The crack depth assumed to be measured at Year 6 is 0.276mm or 0.51mm [74]. Thus, three cases are considered where the crack depth assumes: (a) the original value of 0.11, (b) an SHM/CM measured value of 0.276mm, and then (c) SHM/CM measured value of 0.51mm.

Also presented in the figure is the reliability threshold with a value of 3.71. It can be inferred from this figure that: (i) the updated reliability index curve plotted for cases (b) and (c) are both lower than the case (a), respectively; (ii) a larger crack depth yields lower reliability; (iii) the inspection time calculated for cases (a), (b), and (c) is 9.68, 8.34 and 8.10 years, respectively. From the foregoing, it can be inferred that the reliability index β is sensitive to the initial crack size a_i. Hence, the measured SHM/CM stress, as well as crack size, are valuable data for updating the fatigue RI using the FM approach, achieving an optimised inspection plan and saving OPEX of OWT support structures [17].

5   Conclusion

In this work, S-N curve and FM approaches to fatigue reliability assessment were compared. A 3D parametric FEA model of OWT jacket support structures was developed, taking account of soil-structure interactions. In the FM approach, another FEA model of a curved plate was developed to simulate a part of the welded joint representing the failure–critical hot-spot location where the most cumulative fatigue damage occurs. A number of stochastic FEA simulations of the OWT were performed considering stochastic variables such as environmental and aerodynamic loads as well as soil properties. In the S-N curve approach, an ANN RSM was developed such that the result obtained from the 3D FEA simulations are used to derive the performance function expressed in terms of important stochastic variables. Whereas in the FM approach, this was achieved by linking the two FEA models developed via a second ANN developed for the surrogate modelling. Subsequently, the FORM is applied for both methods in calculating the fatigue reliability index of the structure. The results of the fatigue reliability assessment whilst comparing with the S-N curve approach revealed that the FM approach was optimistic at the beginning while it was found to be more conservative towards the end of the through-life of the structure. It can be concluded that the S-N approach should be used during the design stage, while the FM approach should be used as the structure approaches failure. Sensitivity

studies were performed to investigate the effect of COVs of the random parameters involved in the model on the structure's response. The results revealed a strong dependence of the reliability index on the COV of the material constants. This signifies that apart from their magnitudes, the uncertainties of the crack growth law constants are critical factors that can radically change the structure's reliability performance. Applying the S-N curve approach, the impact of assuming correlation between structural design parameters on the reliability performance of the OWT support structure was elucidated. The reliability index values calculated was found to decrease as the percentage correlation increases. Furthermore, other fatigue reliability assessment exercise performed include estimating the threshold inspection time for the support structure determined via updating the developed reliability framework with assumed SHM/CM data. Hence, the updated reliability assessment provides valuable information for making decisions with respect to the IMR of OWT jacket support structures. Also, the fatigue reliability index calculated assuming a correlation between both segments of the crack growth law from the bilinear FM approach is sensitive to the initial crack depth, and a larger initial crack size leads to lower reliability.

Data availability

The data presented in this study are available on request from the corresponding author. The data and codes are not publicly available because it also forms part of an ongoing study.

Acknowledgement

References

[1]   EWEA. Wind energy scenarios for 2030 2015.

[2]   Kolios A, Mytilinou V, Lozano-Minguez E, Salonitis K. A Comparative Study of Multiple-Criteria Decision-Making Methods under Stochastic Inputs. Energies 2016;9:566. https://doi.org/10.3390/en9070566.

[3]   Collu M, Kolios AJ, Patel M. A Multi-Criteria Decision Making Method to Compare Available Support Structures for Offshore Wind Turbines Platforms for Tidal Energy Converters View project HOME Offshore (http://homeoffshore.org) View project. 2010.

[4]   Kolios A, Wang L, Mehmanparast A, Brennan F. Determination of stress concentration factors in offshore wind welded structures through a hybrid experimental and numerical approach. Ocean Eng 2019;178:38–47. https://doi.org/10.1016/j.oceaneng.2019.02.073.

[5]   Damiani R, Song H. A Jacket Sizing Tool for Offshore Wind Turbines within the Systems Engineering Initiative. Offshore Technol. Conf. OTC 24140, Houston, Texas, USA: 2013. https://doi.org/10.4043/24140-MS.

[6]   Damiani RR, Song H, Robertson AN, Jonkman JM. Assessing the Importance of Nonlinearities in the Development of a Substructure Model for the Wind Turbine CAE Tool FAST. Vol 8 Ocean Renew Energy 2013;8:V008T09A093. https://doi.org/10.1115/OMAE2013-11434.

[7]   Shittu AA. Structural reliability assessment of complex offshore structures based on non-intrusive stochastic methods. Cranfield University, 2020.

[8]   Shittu AA, Kolios A, Mehmanparast A. A Systematic Review of Structural Reliability Methods for Deformation and Fatigue Analysis of Offshore Jacket Structures. Met 2021, Vol 11, Page 50 2020;11:50. https://doi.org/10.3390/MET11010050.

[9]   Ayala-uraga E, Moan T. Fatigue reliability-based assessment of welded joints applying consistent fracture mechanics formulations. Int J Fatigue 2007;29:444–56. https://doi.org/10.1016/j.ijfatigue.2006.05.010.

[10]   Dong W, Moan T, Gao Z. Fatigue reliability analysis of the jacket support structure for offshore wind turbine considering the effect of corrosion and inspection. Reliab Eng Syst Saf 2012;106:11–27. https://doi.org/10.1016/j.ress.2012.06.011.

[11]   Yeter B, Garbatov Y, Soares CG. Fatigue reliability of an offshore wind turbine supporting structure accounting for inspection and repair. In: Soares G, Shenoi E, editors. Anal. Des. Mar. Struct., London, UK: Taylor & Francis Group; 2015, p. 737–747.

[12]   BS 7910. BSI Standards Publication Guide to methods for assessing the acceptability of flaws in metallic structures. BSI Stand Publ 2015:490.

[13]   Silva JE, Garbatov Y, Guedes Soares C. Reliability assessment of a steel plate subjected to distributed and localized corrosion wastage. Eng Struct 2014;59:13–20. https://doi.org/10.1016/j.engstruct.2013.10.018.

[14]   Kim DH, Lee SG. Reliability analysis of offshore wind turbine support structures under extreme ocean environmental loads. Renew Energy 2015;79:161–6. https://doi.org/10.1016/j.renene.2014.11.052.

[15]   Gholizad A, Golafshani AA, Akrami V. Structural reliability of offshore platforms considering fatigue damage and different failure scenarios. Ocean Eng 2012;46:1–8. https://doi.org/10.1016/j.oceaneng.2012.01.033.

[16]   Wang L, Kolios A. A generic framework for reliability assessment of offshore wind turbine monopiles. In: Guedes Soares C, Garbatov Y, editors. Prog. Anal. Des. Mar. Struct. - Proc. 6th Int. Conf. Mar. Struct. MARSTRUCT 2017, Lisbon, Portugal: Taylor and Francis Group; 2017, p. 931–8. https://doi.org/10.1201/9781315157368-105.

[17]   Kolios A, Wang L. Advanced reliability assessment of offshore wind turbine monopiles by combining reliability analysis method and SHM / CM technology, 2018, p. 1412–9.

[18]   Kolios A, Di Maio LF, Wang L, Cui L, Sheng Q. Reliability assessment of point-absorber wave energy converters. Ocean Eng 2018;163:40–50. https://doi.org/10.1016/j.oceaneng.2018.05.048.

[19]   Kolios A. A multi-configuration approach to reliability based structural integrity assessment for ultimate strength. Cranfield University, 2010.

[20]   Jiang Z, Hu W, Dong W, Gao Z, Ren Z. Structural reliability analysis of wind turbines: A review. Energies 2017;10:1–25. https://doi.org/10.3390/en10122099.

[21]   Shittu AA, Mehmanparast A, Shafiee M, Kolios A, Hart P, Pilario K. Structural reliability assessment of offshore wind turbine support structures subjected to pitting corrosion-fatigue: A damage tolerance modelling approach. Wind Energy 2020;23:2004–26. https://doi.org/10.1002/we.2542.

[22]   Wang L, Kolios A, Delafin P-L, Nishino T, Bird T. Fluid structure interaction modelling of a novel 10MW vertical-axis wind turbine rotor based on computational fluid dynamics and finite element analysis. Eur Wind Energy Assoc Annu Conf Exhib 2015, EWEA 2015 - Sci Proc 2015;44.

[23]   Wang L, Quant R, Kolios A. Fluid structure interaction modelling of horizontal-axis wind turbine blades based on CFD and FEA. J Wind Eng Ind Aerodyn 2016;158:11–25. https://doi.org/10.1016/j.jweia.2016.09.006.

[24]   Wang L, Kolios A, Nishino T, Delafin PL, Bird T. Structural optimisation of vertical-axis wind turbine composite blades based on finite element analysis and genetic algorithm. Compos Struct 2016;153:123–38. https://doi.org/10.1016/j.compstruct.2016.06.003.

[25]   Gentils T, Wang L, Kolios A. Integrated structural optimisation of offshore wind turbine support structures based on finite element analysis and genetic algorithm. Appl Energy 2017;199:187–204. https://doi.org/10.1016/j.apenergy.2017.05.009.

[26]   Shittu AA, Mehmanparast A, Wang L, Salonitis K, Kolios A. Comparative Study of Structural Reliability Assessment Methods for Offshore Wind Turbine Jacket Support Structures. Appl Sci 2020;10. https://doi.org/10.3390/app10030860.

[27]   Ivanhoe RO, Wang L, Kolios A. Generic framework for reliability assessment of offshore wind turbine jacket support structures under stochastic and time dependent variables. Ocean Eng 2020;216:107691. https://doi.org/10.1016/j.oceaneng.2020.107691.

[28]   Yeter B, Garbatov Y, Guedes Soares C. Uncertainty analysis of soil-pile interactions of monopile offshore wind turbine support structures. Appl Ocean Res 2019;82:74–88. https://doi.org/10.1016/j.apor.2018.10.014.

[29]   Jung S, Kim SR, Patil A, Hung LC. Effect of monopile foundation modeling on the structural response of a 5-MW offshore wind turbine tower. Ocean Eng 2015;109:479–88. https://doi.org/10.1016/j.oceaneng.2015.09.033.

[30]   DNV GL AS. DNVGL-ST-0126 : Support structures for wind turbines. Høvik, Norway: Det Norske Veritas; 2016. https://doi.org/10.1016/j.biomech.2014.11.025.

[31]   Martinez-Luengo M, Kolios A, Wang L. Structural health monitoring of offshore wind turbines: A review through the Statistical Pattern Recognition Paradigm. Renew Sustain Energy Rev 2016;64:91–105. https://doi.org/10.1016/j.rser.2016.05.085.

[32]   Chojaczyk AA, Teixeira AP, Neves LC, Cardoso JB, Guedes Soares C. Review and application of Artificial Neural Networks models in reliability analysis of steel structures. Struct Saf 2015;52:78–89. https://doi.org/10.1016/j.strusafe.2014.09.002.

[33]   Hosni Elhewy A, Mesbahi E, Pu Y. Reliability analysis of structures using neural network method. Probabilistic Eng Mech 2006;21:44–53. https://doi.org/10.1016/J.PROBENGMECH.2005.07.002.

[34]   Cardoso JB, de Almeida JR, Dias JM, Coelho PG. Structural reliability analysis using Monte Carlo simulation and neural networks. Adv Eng Softw 2008;39:505–13.

[35]   De Santana Gomes WJ. Structural Reliability Analysis Using Adaptive Artificial Neural Networks.

ASCE-ASME J Risk Uncertain Eng Syst Part B Mech Eng 2019;5. https://doi.org/10.1115/1.4044040.

[36]   Ziegler L, Muskulus M. Comparing a fracture mechanics model to the SN-curve approach for jacket-supported offshore wind turbines: Challenges and opportunities for lifetime prediction. Proc. ASME 2016 35th Int. Conf. Ocean. Offshore Arct. Eng. OMAE2016, June 19-24, Busan, South Korea: American Society of Mechanical Engineers (ASME); 2016, p. 1–10.

[37]   Yeter B, Garbatov Y, Soares CG. Reliability of Offshore Wind Turbine Support Structures Subjected to Extreme Wave-Induced Loads and Defects. Proc. ASME 2016 35th Int. Conf. Ocean. Offshore Arct. Eng., Busan, South Korea: 2016.

[38]   Yeter B, Garbatov Y, Guedes Soares C. System reliability of a jacket offshore wind turbine subjected to fatigue. Proc. 5th Int. Conf. Mar. Struct. MARSTRUCT, Lisbon: 2017, p. 939–50.

[39]   Yeter B, Garbatov Y, Soares CG. Risk-based maintenance planning of offshore wind turbine farms. Reliab Eng Syst Saf 2020;202:107062. https://doi.org/10.1016/j.ress.2020.107062.

[40]   Rajasankar J, Iyer N, Rao TA. Structural integrity assessment of offshore tubular joints based on reliability analysis. Int J Fatigue 2003;25:609–19. https://doi.org/10.1016/S0142-1123(03)00021-5.

[41]   Zaheer MM, Islam N. Reliability analysis of universal joint of a compliant platform. Fatigue Fract Eng Mater Struct 2010;33:408–19. https://doi.org/10.1111/j.1460-2695.2010.01453.x.

[42]   Zaheer MM, Islam N. Fatigue and Fracture Reliability of Articulated Tower Joint Under Random Loading. Proc. ASME 2009 28th Int. Conf. Ocean. Offshore Arct. Eng. May 31 - June 5, Pap. Number OMAE2009-79360, Honolulu, Hawaii, USA: American Society of Mechanical Engineers (ASME); 2009.

[43]   Shi P, Mahadevan S. Damage tolerance approach for probabilistic pitting corrosion fatigue life prediction. Eng Fract Mech 2001;68:1493–507. https://doi.org/10.1016/S0013-7944(01)00041-8.

[44]   Melchers R, Andre T. Structural reliability analysis and prediction. 3rd ed. Hoboken, USA: Wiley; 2018.

[45]   Nowak AS, Collins KR. Reliability of Structures. Second Edi. CRC Press; 2012.

[46]   Ayyub BM, McCuen RH. Probability, Statistics, and Reliability for Engineers and Scientists. Third. 6000 Broken Sound Parkway NW, Suite 300, Boca Raton: Taylor and Francis Group; 2011. https://doi.org/10.1201/b12161.

[47]   (DNV) Det Norske Veritas. Fatigue Design of Offshore Steel Structures. Recomm Pract DNV-RPC203 2010.

[48]   DNV. DNV-OS-J101 Design of Offshore Wind Turbine Structures. May 2014:212–4.

[49]   Anderson TL. Fracture Mechanics Fundamentals and Applications. Taylor and Francis; 2005.

[50]   Newman JC, Raju IS. An empirical stress-intensity factor equation for the surface crack. Eng Fract Mech 1981;15:185–92. https://doi.org/10.1016/0013-7944(81)90116-8.

[51]   ANSYS. White Paper: SMART Fracture. 2018.

[52]   Pook LP. Linear elastic fracture mechanics for engineers : theory and applications. WIT Press; 2000.

[53]   Kühn M. Dynamics and Design Optimization of Offshore Wind Energy Conversion Systems. 1999.

[54]   Martinez-Luengo M, Kolios A, Wang L. Parametric FEA modelling of offshore wind turbine support structures: Towards scaling-up and CAPEX reduction. Int J Mar Energy 2017;19:16–31. https://doi.org/10.1016/j.ijome.2017.05.005.

[55]   Drucker D, Prager W. Soil mechanics and plastic analysis or limit design. Q Appl Math 1952;10:157–65.

[56]   Damiani R. JacketSE : An Offshore Wind Turbine Jacket Sizing Tool Theory Manual and Sample Usage with Preliminary Validation. Denver West Parkway Golden, CO: 2016.

[57]   IEC. IEC 61400-1: Wind Turbines Part 1: Design Requirements 2005.

[58]   Sarpkaya TS. Wave Forces on Offshore Structures. Cambridge: Cambridge University Press; 2010. https://doi.org/10.1017/CBO9781139195898.

[59]   Richmond M, Antoniadis A, Wang L, Kolios A, Al-sanad S, Parol J. Evaluation of an offshore wind farm computational fluid dynamics model against operational site data. Ocean Eng 2019;193:106579. https://doi.org/10.1016/j.oceaneng.2019.106579.

[60]   Popko W, Vorpahl F, Zuga A, Kohlmeier M, Jonkman J, Robertson A, et al. Offshore Code Comparison Collaboration Continuation (OC4), Phase I - Results of Coupled Simulations of an Offshore Wind Turbine with Jacket Support Structure. Proc. Twenty-second Int. Offshore Polar Eng. Conf. June 17–22, Rhodes, Greece: International Society of Offshore and Polar Engineers (ISOPE); 2012, p. 337–46.

[61]   Shittu AA, Mehmanparast A, Amirafshari P, Hart P, Kolios A. Sensitivity analysis of design parameters for reliability assessment of offshore wind turbine jacket support structures. Under Rev 2020.

[62]   BSI. BS EN 1990 Eurocode: Basis of Structural Design. Br Stand Inst 2002.

[63]   (DNV) Det Norske Veritas. Structural Reliability Analysis of Marine Structures. DNV CN 30-6 1992.

[64]   Velarde J, Kramhøft C, Sørensen JD. Global sensitivity analysis of offshore wind turbine foundation fatigue loads. Renew Energy 2019;140:177–89. https://doi.org/10.1016/j.renene.2019.03.055.

[65]   Igwemezie V, Mehmanparast A. Waveform and frequency effects on corrosion-fatigue crack growth behaviour in modern marine steels. Int J Fatigue 2020;134:105484. https://doi.org/10.1016/j.ijfatigue.2020.105484.

[66]   Teixeira R, O'Connor A, Nogal M. Probabilistic sensitivity analysis of offshore wind turbines using a transformed Kullback-Leibler divergence. Struct Saf 2019;81:101860. https://doi.org/10.1016/j.strusafe.2019.03.007.

[67]   Reh S, Beley JD, Mukherjee S, Khor EH. Probabilistic finite element analysis using ANSYS. Struct Saf 2006;28:17–43. https://doi.org/10.1016/j.strusafe.2005.03.010.

[68]   ANSYS. DesignXplorer User's Guide 2018.

[69]   Larrosa NO, Akid R, Ainsworth RA. Corrosion-fatigue: a review of damage tolerance models. Int Mater Rev 2018;63:283–308. https://doi.org/10.1080/09506608.2017.1375644.

[70]   Li SX, Akid R. Corrosion fatigue life prediction of a steel shaft material in seawater. Eng Fail Anal 2013;34:324–34. https://doi.org/10.1016/j.engfailanal.2013.08.004.

[71]   Igwemezie V, Mehmanparast A, Kolios A. Materials selection for XL wind turbine support structures: A corrosion-fatigue perspective. Mar Struct 2018;61:381–97. https://doi.org/10.1016/j.marstruc.2018.06.008.

[72]   Adedipe O, Brennan F, Kolios A. Review of corrosion fatigue in offshore structures: Present status and challenges in the offshore wind sector. Renew Sustain Energy Rev 2016;61:141–54. https://doi.org/10.1016/j.rser.2016.02.017.

[73]   Adedipe O, Brennan F, Mehmanparast A, Kolios A, Tavares I. Corrosion fatigue crack growth mechanisms in offshore monopile steel weldments. Fatigue Fract Eng Mater Struct 2017;40:1868–81. https://doi.org/10.1111/ffe.12606.

[74]   Xie R, Chen D, Pan M, Tian W, Wu X, Zhou W, et al. Fatigue Crack Length Sizing Using a Novel Flexible Eddy Current Sensor Array. Sensors 2015;15:32138–51. https://doi.org/10.3390/s151229911.